The *Hubble Space Telescope* Extragalactic Distance Scale Key Project. X. The Cepheid Distance to NGC 7331[1]

Shaun M. G. Hughes
Royal Greenwich Observatory, Madingley Road, Cambridge CB3 0EZ, UK; hughes@ast.cam.ac.uk

Mingsheng Han
University of Wisconsin ~ adison, Wisconsin 53706, USA; han@adcode.astro.wisc.edu

John Hoessel
University ∪ Wisconsin, Madison, Wisconsin 53706, USA; hoessel@uwfpc.astro.wisc.edu

Abi Saha
Space Telescope Science ns.itute, 3700 San Martin Drive, Baltimore, ~ . 21218; saha@stsci.edu

Nancy Silbermann
NASA/IPAC Extragalactic Database, Infrared Processing and Analysis Center, California nstitute ∪ Technology, Pasadena, CA 91125; nancys@ipac.caltech.edu

Peter B. Stetson
)ominion Astrophysical Observatory, 5071 W. Saanich Rd., Victoria BC V8X 4M6;
peter.stetson@hia.nrc.ca

Wendy L. Freedman
The Observatories, Carnegie Institution of Washington, Pasadena CA ≥ 01 wendy@ociw.edu

Paul Harding
Steward Observatory, University ∪ Arizona, Tucson AZ 85721; harding@as.arizona.edu

Robert C. Kennicutt Jnr
Steward Observatory, University of Arizona, Tucson, AZ 85721; robk@as.arizona.edu

Barry F. Madore
NASA/IPAC Extragalactic Database, Infrared Processing and Analysis Center, California Institute of Technology, Pasadena, CA 91125; barry@ipac.caltech.edu

Jeremy. R. Mould
Mount Stromlo & Siding Spring Observatories, Australian National Jniversity, Canberra, Australia;
jrm@merlin.anu.edu.au

Laura Ferrarese
Palomar Observatory, California Institute of Technology, Pasadena, CA 9 125;
ferrarese@deimos.caltech.edu

Holland Ford
)ept of Physics & Astronomy, Bloomberg 501, Johns Hopkins Univ., 3400 N. Charles St., Baltimore, MD 21218; ford@stsci.edu

John A Graham

[1]Based on observations with the NASA/ESA *Hubble Space Telescope*, obtained at the Space Telescope Science Institute, which is operated by AURA, Inc. under NASA Contract No. NAS 5-26555.

Department of Terrestrial Magnetism, Carnegie Institution of Washington,
5241 Broad Branch Rd. N. W., Washington D. C. 20015; graham@jag.ciw.edu

Robert hill
Laboratory for Astronomy & Solar Physics, NASA Goddard Space Flight Center, Greenbelt, MD 20771;
hill@noether.gsfc.nasa.gov

John Huchra
Harvard College, Center for Astrophysics, 60 Garden Street Cambridge, MA 02138;
huchra@cfa.harvard.edu

Garth D. Illingworth
Lick Observatory, University of California, Santa Cruz, CA 950G4;g(li(llJcolick.erg;

Randy Phelps
The Observatories, Carnegie Institution of Washington, Pasadena, CA 91101; phelps@ociw.edu

Shoko Sakai
NASA/IPAC Extragalactic Database, Infrared Processing and Analysis Center, California Institute of
Technology, Pasadena, CA 91125; shoko@ipac.caltech.edu

ABSTRACT

The distance to NGC 7331 has been derived from Cepheid variables observed with HST/WFPC2, as part of the Extragalactic Distance Scale Key Project. Multi-epoch exposures in F555W ($\sim$ V) and 1!'$14W' ($\sim I$), with photometry derived independently from DoPHOT and DAOPHOT/ALLFRAME programs, were used to detect a total of 14 reliable Cepheids, with periods between 11 and 42 days. The I, V - *I* color-magnitude diagram shows all but one of the Cepheids lie within the instability strip, and their period-luminosity relations in *V* and *I* are consistent with those for Cepheids in the LMC. The relative distance modulii between NGC 7331 and the LMC, derived from the V and I magnitudes, infer an extinction to NGC 7331 of $A_V = 0.39 \pm 0.15$ mag, and a reddening-corrected distance modulus to NGC 7331 of 30.92 ± 0.18 mag, equivalent to a distance of $15.3: {}^{1.3}_{1.2}$ Mpc.

Subject headings: Cepheids - galaxies: distances and redshifts galaxies: individual (NGC 7331) stars: early type stars: luminosity function - techniques: photometric

1. Introduction

The *Hubble Space Telescope (HST)* Extragalactic Distance Scale Key Project aims to obtain Cepheid distances 10 $\sim$20 galaxies out to Virgo and Fornax, to use these to calibrate secondary distance estimators, and thereby measure H_0 to an external accuracy of IO%. NGC 7331 (Figure ??) was chosen primarily as a calibrator for the luminosity-line width relation (also known as the Tully-Fisher relation). It lies in the constellation of Pegasus, at position $\alpha = 22\ 37\ 05.2$, $\delta = +34\ 25\ 10$ (J2000), and has a Galactocentric velocity of +1035 km/s (de Vaucouleurs et al. 1991). According to Garcia (1993), NGC 7331 is the dominant member of a group with three other galaxies:[2] UGC12082, NGC 7320A, and UGC12060, which, relative to NGC 7331, are all within 1.7° 011 the sky and $\pm$62 km/s radial velocities.

In many ways NGC 7331 is a twin of the Andromeda Galaxy M31. It has the same early type spiral classification of Sb(rs)I-II in the Revised Shapley Ames scheme by Sandage & Bedke (1985) (and a Hubble type T = 3 by de Vaucouleurs et al. 1991), a very similar inclination of $\sim$75° (estimates vary from 71° by Huchtmeier & Richter 1989 to 75 $\pm$5° by Marcelin et al. 1994 and 74.8 $\pm$ 2.0° by Begeman 1987). The H I rotation curve for NGC 7331 is very regular, and peaks at $\sim$250 km/s (Rubin et al. 1965), and the W_{20} H I 21 cm linewidth is 531:110 km/s (Fisher & Tully 1981) and 536 km/s (measured from Begeman 1987), both also very similar to M31 The properties of being a regular spiral of moderately large inclination make NGC 7331 an ideal calibrator for the luminosity-line width (Tully-Fisher) relation.

We present here the distance to NGC 7331 , using observations obtained with the post-repair mission Wide Field and Planetary Camera (WFPC2) on HST with the F555W and F814W fillers (see Holtzman et al. 1995a and the current version of the WFPC2 Instrument Handbook from STScI for details of the performance of WFPC2). Our methodology follows that used in previous papers in this series: eg M100 (Ferrarese et al. 1996), M101 (Kelson et al. 1996), NGC 925 (Silbermann et al. 1996), NGC 3351 (

[2] Garcia also claimed NGC 7363 to be a member of this group, but it's velocity is almost 6000 km/s greater, and probably forms a background group with NGC 7320B and NGC 7320C. As well, Tonry et al. (1996) also include NGC 7457 as a member, but at a distance on the sky of 6.6°, this would make it a rather loose group.

Graham et al. 1996), and NGC 3621 (Rawson et al. 1996). Photometry was obtained with DoPHOT and ALLFRAME (§ ??), to identify and measure periods and luminosities of 14 Cepheid variables (§ ??), applying the calibrations described in Ferrarese et al. (1996) and Hill et al. (1996). Period-luminosity relations were fitted to these Cepheids, relative to the Large Magellanic Cloud (LMC), to derive reddening-corrected distance moduli for each photometry set (§ ??). Implications for the properties of NGC 7331, and previous calibrations of the Tully-Fisher (TF) relation (§ ??) are briefly discussed. Preliminary results of this work were described in Hughes, Han & Hoessel (1996).

2. Photometry

The WFPC2 field lies 3.5 arcmin north of the galaxy's nucleus, along the major axis (Figure ??). Variable stars were detected from 15 epochs of F555W cosmic ray-split exposures, and their colors were measured from 4 epochs of F814W exposures, over the interval of 1994 June 18 to 1995 August 17, as listed in Table ??. Each cosmic ray-split exposure pair consisted of a 1600 sec and a 1200 sec exposure (except for epoch 7 and the F814W exposure in epoch 8, where the 1600 sec exposures were missed due to safing events), with a gain of 7 e^-/DN and a readout noise of 7 e^-. All of these epochs were taken after the decrease in the WFPC2 operating temperature (which occured on 1994 April 23). Although there appears to be a charge transfer inefficiency effect in the WFPC2 CCDs, this is only seen in exposures with a low background, and is negligible for high backgrounds (brighter than 70e^-) (Rawson et al. 1996). As our NGC 7331 frames all have backgrounds brighter than 70 e^-, they should not have been affected. Two short exposures of 260 sec in F555W and F814W were also made at epoch 13, but have not been used as they were intended for calibration backup via ground-based observations in case there were any problems with the photometric calibrations.

The science frames were processed through the standard STScI pipeline (Holtzman et al. 1995a). The photometric distortions introduced by the WFPC2 corrective optics were rectified by multiplying each image by a pixel area correction map. These differ slightly from those used by Holtzman et al. (1995b) in that the normalization is relative to the median pixel, rather than the largest. Pixels either off the WFPC2 pyramid surface, or vignetted by the pyramid edge, were set to saturation, and subsequently ignored by the photometry programs.

The photometry was derived using programs based on DoPHOT (Schechter, Mateo & Saha 1993; Saha et al. 1994) and DAOPHOT/ALLFRAME (Stetson 1994), in a similar way as described in detail for M100 by Ferrarese et al. (1996) and Hill et al. (1996), adopting the long exposure calibration (see Appendix).

2.1. DoPHOT

DoPHOT measures magnitudes by fitting a purely analytic point-spread function (PSF) to objects detected above a user-specified threshold. For DoPHOT, each cosmic ray-split pair of observations were firstly combined using an algorithm developed by AS, to produce single frames per epoch mostly free of cosmic rays. This program compares the two input frames on a pixel-by-pixel basis (after correcting for exposure times). If one pixel is greater than the other by more than 4-sigma, then the lower pixel value is taken as the true value, otherwise the mean is adopted. If a cosmic ray event has been detected, then the sigma threshold decreases to 2-sigma for the nearest neighbor pixels. (Because the PSF is under-sampled by the pixels, great care needs to be taken to ensure that cosmic-ray removal algorithms don't also remove

the tops of stars. For exa1 nple, initially a 3-sigma threshold was used, which subsequently was found to have significantly affected the DoPHOT photometry.) The cosmic ray-cleaned images were run through DoPHOT, to obtain the positions of the brightest stars, which were then matched (using DAOMATCH and DAOMASTER, Stetson 1994) to obtain the coordinate transformations between epochs. The X and Y offsets were all less than $\sim$ 0.2 arcsec. All the frames for each chip were then median-combined to produce clean and reasonably deep master images, which were then passed through DoPHOT, to produce a master list of objects, retaining only those objects DoPHOT classifies as stars. This produced 6701,7621,8048 and 8953 stellar objects in chips 1-4, respectively. The coordinates of the master list were then transformed to the positions of each ep och, and each of these lists were used within DoPHOT to obtain raw DoPHOT photometry of each of the master list, objects in each of the epoch frames.

The raw photometry was then calibrated to equivalent 0.5 arcsec aperture mags, using aperture corrections and measured zero-J)oirltsforl)c)tll filters andeachchip (scc Appendix A). The photometry of all epochs for each object, now calibrated to 0.5 arcsec aperture mags, was then combined using DAOMASTER, to produce a lightcurve for every object in the input master list, The mean 0.5 arcsec aperture mags ($F555W_{0.5}$ and $F814W_{0.5}$) were then converted to Johnson V and Kron-Cousins 1 photometry using the zero points and color transforms in Appendix A (and obtained from Holtzman c1 al. 1995b).

2.2. ALLFRAME

For ALLFRAME, the original science frames were used (i.e. treating each of the cosmic ray-split exposures as two individual epochs), following the ALLFRAME method described for previous galaxies in this series (eg. Ferrarese et al. 1996; Silbermann et al. 1996). The DAOPHOT/ALLFRAME program (Stetson 1994) takes a different approach in doing the photom etry, in that an analytic PSF is augmen ted by an empi rically- determined difference map, which represents the intensity-weighted mean difference between the observed PSF of a large sample of isolated stars and the analytic function. The PSF is also allowed to vary as a quadratic function of position on the chip, to account for variat ions in the PSF across each chip. In the case of the HST images of NGC 7331, there were too few isolated stars to adequately characterize the PSF, so the PSFs derived from a number of independent images of globular cluster fields by PBS were used. ALLFRAME then fits these PSFs (one per filter and chip) to all st ars on all the frames. To do this, ALLFRAME must first have a master input list of objects, which like DoPHOT, was derived from median images produced from coordinate transformatio ns defined by matches (again using DAOMATCH and DAOMASTER) of bright isolated stars on each of the indiv id ual cosmic ray-cleaned frames. The difference with DoPHOT is that ALLFRAME only uses this s tarlist as a starting point, and uses the results of simultaneous PSF fitt ing on all the frames to tweak the coordinate transformations between frames, thereby iteratively improving the master list, and making maximum use of the available in formation. The final photometry files produced by ALLFRAME for each epoch were then matched using DAOM ASTER, to produce a single file contain ing the posi tions and magnitudes of all the m atched stars at all the epochs. This produced 875, 5248, 2807, and 10677 objects in chips 1-4, respectively.

The aperture corrections were adopted from the mean corrections of other galaxies in this series, as listed in Appendix I. As for DoPHOT, these ().5 arcsec aperture mags were then converted to Johnson V and Kron-Cousins 1 using the transfo rmations of Holtzma n et al. (1995b).

2.3. Comparison Between DoPHOT and ALLFRAME Photometry

A comparison between mean calibrated DoPHOT and ALLFRAME mags is given in Figure ??, which is the difference between calibrated mean DoPHOT and ALLFRAME 11 ST magnitudes (i.e. $F555W_{0.5}$ and $F814W_{0.5}$) of all stars, matched to within a 0.5 pixel radios. While the scatter is large, the stars with the largest scatter also tend to have the largest photometric errors, and tend to be contaminated by near neighbors and/or a bright background. A better comparison would be to match just skins which are isolated and unaffected by cosmic ray events. This selection was achieved by comparing only stars with an rms from all mags of less than 0.1 mag, and which were seen to be isolated, stellar-like objects. To allow easier external comparisons with our calibrated mags, we list in Table ?? the positions and calibrated mean DoPHOT and ALLFRAME magnitudes (V and *I*) of these (reference) stars. Their 11 ST mag differences (in the sense DoPHOT - ALLFRAME) are given in ??. They all agree to within 0.15 mag, with the greatest deviation being WF3. Some of the scatter between these DoPHOT and ALLFRAME magnitudes arises from the different methods used to estimate the local sky. For DoPHOT, the sky is estimated from a weighted average of all pixels within the 9×9 pixel aperture, whereas DAOPHOT/ALLFRAME estimates the sky as the modal value of pixels in a circular annulus (in this case having radii of 2.5 and 25 pixels). As only 90% of the light from a star is contained within a radius of 0.5" (Holtzman et al. 1995b), which is a radius of 5 pixels on the WF chips, both of these sky estimates will be contaminated by the broad wing component of the star being measured, but in different ways. The effect of this contamination will be greatest for the bright stars in Table ??, but will be minimal, when compared to the background, for stars of Cepheid magnitudes.

Therefore, an even more relevant comparison, in terms of the distance to NGC 7331, is the difference in the calibrated Cepheid magnitudes (see § ??), which are reflected in the differences between the Period-Luminosity fits in Table ??. This infers that the DoPHOT and ALLFRAME calibrated mags agree to ~0.08 mag in *V* and ~0.03 mag in *I*, a difference of one sigma with respect to the internal errors, and well within the external errors.

3. The Cepheids

To detect the variables, the objects in the DoPHOT photometry sets were firstly grouped into magnitude bins of width 0.5 mag. A variable was then defined as any object with a robust rms-like dispersion (the F-σ parameter, based on the inner range of variability, as described in Hughes 1989, and derived from Hoaglin, Mosteller & Tukey 1983) greater than twice the mean rms of its magnitude bin. Each object was also required to have been matched in at least 10 epochs. These variables were then searched for periodicity with periods between 10 and 80 days, using a program based on the Phase Dispersion Minimization (PDM) algorithm of Stellingwerf (1978), which is based on the Lafler & Kinman (1965) statistic. The main advantage of this method is that it is efficient at detecting periodicity in small epoch samples, and is insensitive to light curve shape. Simultaneously, the image of each variable was viewed to ensure it was not a spurious variable caused by a close association with another object, and its lightcurve, phased at the optimum PDM period, was also inspected to verify its Cepheid-likeness.

For the ALLFRAME photometry sets, variable candidates were identified using two indicators. The first is similar to the χ^2 parameter of Saha & Hoessel (1990), and the second is the color index parameter of Welch & Stetson (1993). Cepheid candidates were identified by visually examining the phased light curves of the variable candidates. Any epochs contaminated by cosmic rays were removed interactively.

The final list of good Cepheids (Table??) was selected on the basis that each had to appear in both candidate lists. No good Cepheids were found on chip 1 (the PC chip), due to the reduced FOV and photometric errors being much larger at the magnitudes of the Cepheids, compared to the other WF chips (0.25 to 0.6 mag, at magnitudes of 251,027 in V, compared to errors of ().1 to ().3 mag on the WF chips), resulting in much lower yields of variable candidates due to the 2-sigma selection. For Cepheids to have made this cut, they would need to have amplitudes greater than $\sim$ 1 .() mag, and only half the Cepheids in Table ?? have such large amplitudes.

The mean V magnitudes are unweighted intensity averaged means (i.e. - $2.5\log_{10}(\frac{1}{N}\Sigma 10^{-0.4m_i})$), which we use instead of phase-weighted mags, as the distribution of epochs provides well-sampled light curves over all periods between 10 and 60 days, due to the optimized sampling algorithm developed by Freedman et al. (1994a), and the flexible and accurate scheduling capability of HST. For such optimally sampled lightcurves, there is minimal difference between intensity and phase-weighted mags, as verified by Ferrarese et al. (1996) in M100, and Silbermann et al. (1996) in NGC 925. The magnitudes at each epoch of the Table ?? variables are listed in Table ?? (DOPHOT), Table ?? (ALLFRAME), where for Table ??, the cosmic ray-split exposure mags are intensity averaged, to give one magnitude per epoch.

To compensate for the poor sampling of the I data (there were only four epochs), the mean I mags were estimated following the method developed by Freedman (1988) and applied by Ferrarese et al. (1996). This uses the fact that the amplitude in V is almost twice the amplitude in I, hence a well-sampled mean I magnitude $\langle I\rangle_{12}$ (over $\sim$ 12 epochs) will be estimated as $\langle I\rangle_{12} = \langle I\rangle_4 - 0.51(\langle V\rangle_{12} - \langle V\rangle_4)$, where $\langle I\rangle_4$ and $\langle V\rangle_4$ are the intensity averaged I and V magnitudes at those epochs (up to four) where both F555W and F814W images were obtained.

The Cepheids in Table ?? are marked in the deep I vs V - I color-magnitude diagram in Figure ??, derived from the mean magnitudes from all epochs (for clarity, only every 10th star in the CMD is plotted). All of the DoPHOT mag Cepheids lie in the instability strip. We also plot the locus of the blue plume, red supergiant and red giant branch for Shapley Constellation III, shifted in magnitude and color to match the relative distance and extinction of NGC 7331. The position of the red giant branch locus implies our limiting magnitude is too bright to apply the tip of the red giant branch distance method (eg Lee et al. 1993) as a check on our Cepheid distance.

The luminosity function of the blue plume stars (i.e. with V - I < 0.3) is plotted in Figure ??. Before incompleteness (at V > 26), the slope of the luminosity function is 0.61, similar to that of M81 (().57; Hughes et al. 1994), and consistent with other late-type galaxies (Freedman 1985). The luminosity function for stars with Cepheid-like colors (().5 < V - I < 1.5) is also plotted in Figure ??, and shows that incompleteness for Cepheids sets in at V > 27.8 mag, consistent with our faintest Cepheids in Table ??, which have (1'): 27.4 (V8) and (V) = 27.7 (V13, DoPHOT). The degree to which crowding and limiting magnitude affects Cepheid completeness is being investigated via artificial star tests by Ferrarese et al. (in preparation).

The parameters for the good Cepheids in Table ?? are ID, WFPC2 chip, position (both the RA and Dec at equinox 12000, and their X and Y pixel position on each chip), and the periods and intensity averaged V magnitude and V - I color for each of the ALLFRAME and DoPHOT sets. They are identified in the WFPC2 field in Figure ??, as well as in more detailed finding charts in Figure ??, and their lightcurves, phased to the period given in Table ??, are shown in Figure ??. The mean differences between the DoPHOT and ALLFRAME Cepheid data was ΔV = 0.05 mag, with an rms dispersion of ().17 mag, ΔI = 0.03 mag, rms = 0.19 mag, and ΔPeriod = 0.03 days, with an rms dispersion of 1.27 days.

4. The Distance to NGC 7331

To obtain a Cepheid distance, we follow the methodology of previous papers in this series, and fit V and I P-L relations relative to the LMC Cepheids, adopting the distance and reddening to the LMC of 18.5 ± 0.1 mag and $E(V-I) = 0.13$ (i.e. $E(B-V) = 0.10$, $A_V = 3.3E(B-V)$, and use the Cardelli et al. 1989 extinction law $A_I/A_V = 0.7712 - 0.5897/R_V = 0.592$ for $R_V = 3.3$) from Madore & Freedman (1991; hereafter MF91), and fitting the MF91 P-L relations, derived from a set of observations of 32 LMC Cepheids:

$$M_V = -2.76(\pm 0.11)[\log(P) - 1.4] - 5.30(\pm 0.05); rms = 0.27$$

$$M_I = -3.06(\pm 0.07)[\log(P) - 1.4] - 6.09(\pm 0.03); rms = 0.18$$

to obtain V and I distance moduli (μ_V, μ_I). However, recently Tanvir (1996) has re-derived the LMC P-L relations, from a compilation of data from several sources, of 53 LMC Cepheids, and finds they are best fit by P-L relations of the form:

$$M_V = -2.774(\pm 0.083)[\log(P) - 1.4] - 5.262(\pm 0.040); rms = 0.233$$

$$M_I = -3.039(\pm 0.059)[\log(P) - 1.4] - 6.049(\pm 0.028); rms = 0.164$$

There is very little difference in the V P-L relation, but a significant difference in the I P-L relation zero-point. Tanvir has attributed this difference to the fact that MF91 used I magnitudes derived from $<V> - <I>$, rather than intensity means of the I data. If confirmed, this means that use of the MF91 relations would produce a systematic overestimate of the relative I distance modulus of a galaxy by ~ 0.04 mag, hence of the reddening, which produces an overestimate of the reddening-corrected distance modulus of 0.1 mag, and a corresponding underestimate of H_0 by 5%. An ongoing program to measure mean I-band magnitudes for a sample of LMC Cepheids being carried out by us at Las Campanas Observatory and Mount Stromlo will shed further light on this issue. In the meantime, to be consistent with previous papers in this series, we continue to use the MF91 P-L relations.

As can be seen in the image of Figure ?? (and to a more dramatic extent in Figure ??), there are noticeable amounts of dust in NGC 7331, so it is important to measure and account for this as accurately as possible. As in MF91, we measure the mean reddening $E(V-I)$ for the whole sample of Cepheids from the difference $\mu_V - \mu_I$, which is then used to derive the reddening-corrected distance.

We have two methods of fitting the MF91 P-L relations in V and I. The first adopts the LMC P-L relations, using least squares fits at the adopted slopes. The second method, as used by Ferrarese et al. (1996) for M100, takes the same set of LMC Cepheids and adds an offset to their magnitudes that minimizes the scatter when combined with the NGC 7331 Cepheids. Both methods produced virtually identical results, and so we only present the results of the first method. One of the ALLFRAME Cepheids (V13) had a very blue color ($V-I = 0.0$), due to a faint $<V>$ magnitude (relative to that obtained from DoPHOT), which put it outside the instability strip, and was excluded from the ALLFRAME fits. Removing V13 from the DoPHOT fits only reduced the distance modulus by 0.01 mag (method 1) and 0.03 mag (method 2). The P-L relations and the fits using the MF91 slopes are shown in Figure ??.

The number of Cepheids used in the fits, the apparent distance moduli in V and I (μ_V, μ_I), reddenings $E(V-I)$, and reddening-corrected distance moduli μ_0 for each photometry set, are listed in Table ??. The 1-σ uncertainties in μ_V and μ_I are just the errors on the mean from the least squares fits (combined in quadrature with the uncertainties in the LMC P-L fits). Because a component of the scatter in the V and I P-L relations will be correlated, the uncertainty in μ_0 is derived from the dispersion in a Wesenheit

function, $W = V - 2.45(V - I)$, which is adapted to the reddening assumed between V and), as this will implicitly propagate the photometric uncertainties and cancels the differential reddening-induced scatter (Madore 1 982). The uncertainty in μ_0 in Table ?? thus includes the observational uncertainties in the photometry. To search for any zero- point variations between chips, separate fits were also made to each chip. We note that the fits for chip 3 give consistently larger μ_V, for both DoPHOT and ALLFRAME magnitudes, hence larger estimates for the extinction, and so lower estimates for μ_0. Hill et al. (1 996) found similar discrepancies with the WF3 photometry in the M 1OO data, but assumed this was due to the extra crowding (for Ml 00, WF3 was the closest chip to the nucleus). For NGC 7331, WF3 is the least affected by crowding, inferring the cause may be related to the WF3 chip and/or optics. It is also possible that the difference is due to a calibration error in the WF3 magnitudes, but as these were made independently for DoPHOT and ALLFRAME, such an error, if it exists, is more likely to be in the Holtzman et al. (19951,) calibration from 0.5″ apertures to standard mags. However, as there are only three Cepheids on WF3, if there is any systematic error involved, it will have minimal impact on the average derived from all three WF chips. The luminosity function for stars with Cepheid-like colors in Figure ?? showed that we may be affected by incompleteness at the faintest (ie short period) end of the Cepheid distribution. To check for the effects this may have in fitting the PL relations, the lower period limit was also varied, from 10 days (the lower period limit) to 15 and 20 days. There is a small trend to slightly larger distance modulus as the low period limit is increased, from 30.80 LO 30.85 (ALLFRAME) as the low period limit increases from 10 to 25 days, but this is well within the errors, indicating that no strong Malmquist bias is present in our Cepheid sample, and that our distance estimate will not be significantly affected by incompleteness.

A possible complication affecting our distance estimate may be the difference in metallicity between the NGC 7331 and LMC Cepheids. The abundance of our WFPC2 field can be estimated by extrapolating the abundance gradient derived from the inner H II regions by Oey & Kennicutt (1993) of -().1 dex/arcmin. Oey & Kennicutt derive an abundance of log(O /H)= 3,()() at an effective radius R_E = 1,07 arcmin, implying a mean abundance of log(O/ H) = - 3.25 at a radius of 3.5 arcmin. Assuming the LMC Cepheids have log(O/H) = - 3.65 (Dufour 1 990), then these NGC 7331 Cepheids are likely to be 2.5 times more metal rich. However, the Oey & Kennicutt sample only extended to a projected radius on the disk of 79 arcsec, so the extrapolation to our WFPC2 field, at a radius of 3.5 arcmin, is highly uncertain. Kennicutt (private communication) now has observations of 11 11 regions in the WFPC2 field, and preliminary reductions indicate the metallicity is only 1.5 :l ().3 times more metal rich than the LMC. Adopting this metallicity, then the calculations of Chiosi, Wood & Capitanio (1 993) would imply the NGC 7331 Cepheids are only $\sim$ 0.04:1 ().()2 mag fainter in V than those in the LMC (for a mean period of 25 days, and making the same assumptions about color distribution, convective overshoot, and helium dependence on metallicity as Tanvir 1 996). However, there is a smaller change in the I mags, which when folded through the reddening correction, means that the distance modulus reduces by only ().()1 1 :l 0.006 mag. This prediction is consistent with the observational results for M31 (Freedman & Madore 1990), which show no statistically significant evidence for any metallicity effect. We await the analysis of the inner arid outer M101 fields, to see if the theoretical predictions of Chiosi, Wood & Capitanio (1 993) are confirmed. At this stage we therefore simply add this theoretical prediction as a possible systematic error, conservatively estimated as 0.02 mag, in Table ??.

In addition to the uncertainties of the photometry (included in the PL fits), the true distance estimate will also be affected by the systematic uncertainties in the zero-point calibration from HST to ground-based V and I mags, and the LMC distance modulus, as listed in Table ??. The former are assumed to be uncorrelated, and hence must be factored for the ratio of their contributions via the reddening correction: i.e. $\mu_0 = 2.45\mu_I - 1.45\mu_V$, hence $\Delta(ZP) = ((2.45\Delta(ZP)_I)^2 + (1.45\Delta(ZP)_V)^2)^{\frac{1}{2}}$. The contribution to the

total error budget is listed in Table ??, giving a total uncertainty in μ_0 of 0.19 mag for DoPHOT and 0.18 mag for ALLFRAME.

The reddening of $E(V-I) = 0.26$ (DoPHOT), 0.16 (ALLFRAME), implies a mean extinction to NGC 7331 of $A_V = 0.64 \pm 0.15$ (DoPHOT), 0.39 ± 0.15 (ALLFRAME) mag. The foreground Galactic extinction in the direction of NGC 7331 is $A_V = 0.27$ (derived from $E(B-V) = 0.083$ from Burstein & Heiles 1984), thus the mean extinction internal to the NGC 7331 Cepheid field is 0.37 (DoPHOT), 0.12 (ALLFRAME) mag in V. The reddening-corrected distance modulus is 30.803 0.19 (DoPHOT), 30.924 0.18 (ALLFRAME) mag, equivalent to a distance of $14.5^{+1.3}_{-1.2}$ (DoPHOT), $15.3^{+1.3}_{-1.2}$ (ALLFRAME) Mpc. For consistency with previous papers, and for simplicity, we henceforth quote the results based on the ALLFRAME photometry alone.

Previous distance estimates to NGC 7331 are listed in Table ??. The similarities between NGC 7331 and M31 prompted Rubin et al. (1965) to make the earliest approximate distance estimates to NGC 7331 in terms of a ratio of the distance to M31. These estimates convert to 17.7 Mpc, based on comparing recession velocities; and 15.4 Mpc, based on comparing apparent diameters, where we adopt the distance to M31 of 770 kpc from Freedman & Madore (1990). Tully (1988) estimated a velocity distance of 14.3 Mpc based on assuming $H_0 = 75$ km/s/Mpc, and a Virgo-centric infall model of the Local Group of 300 km/s. The Tully-Fisher distance estimates for NGC 7331 are 9.6 Mpc (B band, Bottinelli et al. 1985) and 12 Mpc (I1 band, Aaronson et al. 1982). The only recorded supernova in NGC 7331 was SN1959D, of type II, unfortunately occuring before the era of estimating distances to type II SN from the expanding photospheres method (eg. Schmidt et al. 1994[3]).

5. Discussion

The aim of the Key Project is the measurement of the Hubble Constant by calibration of secondary distance indicators. We consider the impact of our new distance on the calibration of two such distance indicators here.

5.1. The Tully Fisher relation

Mould et al. (1996) have updated the calibration of the infrared Tully Fisher relation, noting the importance of populating the calibration for galaxies of large line width, galaxies which can be detected at large distances, where peculiar velocities are negligible relative to recession velocities. In Figure ?? we add NGC 7331 to Table 4 of Rawson et al. (1996).

We adopt an I1 velocity width of 531 ± 10 km/s (given by Fisher & Tully), an inclination for NGC 7331 of 72°, 3° less than that of Aaronson et al (1982) (*cf.* 73° Tormen & Burstein 1995).

The least squares fit IRTF relation excluding NGC 7331 is $I_{0.5} = -10.0(\pm 2.4)(\log\Delta V - 2.5) - 21.3(\pm 0.3)$, with $\sigma = 0.36$. When we add in NGC 7331 the fit becomes $I_{0.5} = -10.6(\pm 2.2)(\log\Delta V - 2.5) - 21.3(\pm 0.3)$, with $\sigma = 0.39$. Hence this distance to NGC 7331 is consistent with the current IRTF calibration, but it points to a dispersion of 0.4 mag in the relation, not very different from that found by Aaronson & Mould (1982) in groups and clusters.

[3] Although Schmidt et al. list SN1989L as occuring in NGC 7331, this should read NGC 7339.

5.2. Kinematic and Nuclear Properties

The kinematics of NGC 7331 have been extensively analyzed by Bower et al (1993), who were able to fit a constant M/L_V dynamical model, as a function of radius, and found M/L_V = 5.3, assuming a distance of 12 Mpc (from Aaronson et al 1982). Our new distance therefore implies an M/L_V = 4.2, and a total mass of $4.6 \times 10^{11} M_\odot$. This can be compared to M/L_B = 8.1 derived from Fisher & Tully (1981), and a total mass of $4.1 \pm 0.5 \times 10^{11} M_\odot$ (where our distance of 15.3 Mpc implies a Holmberg diameter A_H = 66 kpc, μ_0 = 30.92 implies M_B = -21.42 and $\log L_B$ = 10.76.

Although NGC 7331 looks like a normal early-intermediate type spiral galaxy with a significant bulge, it also has a mildly active (weak LINER) nucleus. Cowan et al (1994) measured its 20cm and 6 cm radio flux to be 234 and 121 μJy, respectively. At a distance of 15.3 Mpc, this makes it 3.4 and 4.8 times the luminosity of Sgr A, at these wavelengths.

5.3. The Virgo-centric flow

We can derive a 'naive' distance estimate based just on NGC 7331's recession velocity. Adopting Tully's (1988) simple Virgo-centric infall model of the Local Group, the Hubble flow velocity for NGC 7331 would then be 1075 km/s, giving H_0 = 70 km/s/Mpc. Unfortunately, such an estimate is prone to systematic errors, by ignoring the likely extra contribution to peculiar velocity provided by the rest of the mass outside the local group and the Virgo cluster, which is why we prefer to use the Cepheid distances as calibrators of secondary distance indicators capable of measuring distances to redshifts where peculiar velocities are comparatively small. Alternatively, the Virgo-centric flow model of Aaronson et al (1982) implies a distance 0.74 times that of the Virgo cluster. Our distance to NGC 7331 would then imply a kinematic distance to Virgo of 20.7 Mpc, compared to a direct Cepheid distance (derived from M100) of 16.1 $\pm$ 3.2 Mpc (Ferrarese et al 1996).

5.4. Surface Brightness Fluctuations

In addition to the TF calibration, the large bulge in NGC 7331 can be used as a calibrator for SBF. Tonry et al. (1996) has adopted a calibration of surface brightness fluctuations

$$\bar{M}_I \quad \bar{M}_{I0} + 4.5\,(V \quad I \qquad 5)$$

At a distance of 14.9 Mpc, the unpublished measurement of a field 1-2 arcmin along the minor axis yields $\bar{M}_{I0}$ = - 2.27 $\pm$ 0.3 mag, significantly brighter than his adopted value of - 1.74 $\pm$ 0.07 mag (Tonry et al. 1996).

Tonry et al take into account the foreground reddening to each of the SBF samples (eg. A_B = 0.33 mag for N7331), but not any internal extinction. For the E and S0 galaxies, and the very edge-on spirals, this may be appropriate, but for N7331 there is evidence from stellar population studies in the bulge by Prada et al (1996) that there is additional reddening internal to the bulge, of $A_V \sim 0.5$ mag, or A_I = 0.3 mag. A quirk of SBF is that taking reddening into account causes $\bar{M}_{I0}$ to become fainter. Hence an extra reddening of A_I = 0.3 would increase the value of $\bar{M}_{I0}$ quoted here, making it more consistent with Tonry's standard value. As well, if there is this much dust in the bulge of NGC 7331 then it may also have a young

stellar component as well. Although the color term in the SBF calibration is intended to allow for such variations, the reddening would tend to mask the bluer colors such a young component would contribute, thus making the deviation from an unreddened old population even greater.

6. Conclusion

We have used 15 epochs of HST F555W frames to produce lightcurves of all stars within the field, to a limiting magnitude of V 28 mag, using two photometry programs (DoPHOT and DAOPHOT/ALLFRAME), and from these lightcurves identified a total of 14 reliable Cepheids in NGC 7331. Using the ALLFRAME data, and an additional 4 epochs of F814W frames, period-luminosity relations derived from LMC Cepheids were fitted to the NGC 7331 Cepheids, to measure a mean reddening of $E(V-I) = 0.16 \pm 0.06$, and a reddening-corrected distance modulus of 30.92 ± 0.18 mag, equivalent to a distance Of $15.3^{+1.3}_{-1.2}$ Mpc.

We are indebted to the very able support provided by the staff at STScI, in particular to Doug Van Orsow for his scheduling abilities. Support for this work was provided by NASA through grant number 2227-87A from STScI which is oI)c.rated by AURA under NASA Contract NAS5-26555. This research has made use of the NASA/IPAC Extragalactic Database (NED) which is operated by JPL, California Institute of Technology, under contract with NASA.

A. Appendix A - Calibration Parameters

The calibration of the raw 1)01' IOT photometry is given by:

HST mag = Raw DoPHOT mag + 30.0 + AC + 2.5*$\log_{10}(t)$ + ZP

where 11 ST mag is the 0″.5 aperture magnitude system ($F555W_{0.5}$ and $F814W_{0.5}$), as defined by Holtzman et al. (1995b), AC is the aperture correction (to correct for the 9×9 pixel square aperture, derived from AS observations of Leo 1), t is the exposure time, in seconds, and Xl is the zero-point (derived by AS from comparing mags obtained from the first epoch NGC 7331 frame with observations of Pal 4, following the prescription of Holtzman et al. 1995b).

The DoPHOT aperture corrections are given by:

AC = C0 + C1*x + C2*y + C3*x*x + C4*y*y + C5*x*y

where x and y are pixel coords of each full (800 x 800)" WFPC2 chip, and the C coefficients are given in Table ??.

For bright stars on a faint background (as for the cluster calibration data), there is a charge transfer efficiency (CTE) effect which produces a ramped offset in the measured magnitudes of ~ 0.05mag/800 pixels in the Y direction (see Holtzman et al. 1995b for details). AS accounted for any systematic error' this may introduce by adding - 0.020 mag to his zero-points. As discussed in Rawson et al (1996), zero-points for WFPC2 also seem to differ by 0.05 mag between short and long exposures (i .e. objects observed with long exposure times appear brighter by 0.05 mag, compared to snort exposure times). For long exposures (i.e. ours) the 1)01'110'1' zero-poi]lts (for a gain of 7) are defined in Table ??.

Because DoPHOT and DAOPHOT have different methods of estimating the sky and different PSF profiles, their calibration to standard magnitudes has to be done independently. '1'0 gain full advantage of this effort, the ALLFRAME calibration was also done using a different data set, bad on short exposures of stars in Galactic globular clusters, to provide an independent check on the calibration procedure. Because ALLFRAME allows the PSF to vary across each chip, its calibration only requires zero-points and a single aperture correction per clli])/filter to convert the raw mags to equivalent 0.5 arcsec aperture mags, where for DAOPHOT/ALLFRAME:

HST mag = Raw ALLFRAME mag + AC + 2.5*$\log_{10}(t)$ + ZP

The zero-points were derived by PBS for each chip and filter from weighted averages of long exposure HST vs ground-based photometry of the clusters ω Cen (Walker 1994), and NGC 2419 and Pal 4 (Bolte & Stetson, private communication). The 11 ST w Cen data were taken with a gain of $\sim$14, and were converted 10 a gain of $\sim$7 using the ratios in Holtzman et al. (1995b). PBS measured a mean CTE ramp effect of 0.010 mag/800 pixels, which was then applied to the input cluster mags. The aperture corrections were derived from mean measurements by PBS of aperture corrections for the two M101 fields and the NGC 4725 field. These, and the zero-points for ALLFRAME (again, on the LONG exposure scale) are given in Table ??.

The 11 ST magnitudes were then transformed to Johnson V or Kron-Cousins I magnitudes, using the transformations derived by Holtzman et al. (1995b):

$V = F555W_{0.5} - 0.045(V - I) + 0.027(V - I)^2$

$I = F814W_{0.5} - 0.067(V - I) + 0.025(V - I)^2$

where the $(V - I)$ colors were estimated from iteration, starting from $F555W_{0.5}$- $F814W_{0.5}$, and ending

when $|V - I - (V - I)| < 0.001$ mag (usually one iteration was sufficient).

REFERENCES

Aaronson, M., *et al.* 1982 ApJS 50, 241

Aaronson, M., Mould, J.R. 1982 ApJ 265, 1

Begeman, K.G. 1987 *PhD thesis*, University of Groningen.

Bottinelli, 1,., *et al.* 1985 A&ASupp 59, 43.

Bower, G. A., Richstone, D.O., Bothun, G.D., Heckman, T.M. 1993 ApJ 402, 76.

Burstein, D., Heiles C. 1984 ApJS 54, 33.

Cardeli, J.A., Clayton, G.C., Mathis, J.S. 1989 ApJ 345, 245.

Chiosi, C., Wood, P.R., Capitanio, N. 1993 ApJS 86, 541.

Cowan, J.J. Romanishin, w., Branch, D. 1994 ApJ 436, L139.

de Vaucouleurs, G., de Vaucouleurs, A., Corwin, 11., Buta, R., Paturel, A., Fouqué, P. 1991 *Third Reference Catalogue of Bright* Galaxies (Berlin: Springer).

1)ufour, R. 1990 in *Symp. on Evolution in* Astroplly.sits, ESASP-31 O

Ferrarese, L. *et al.* 1996 ApJ 464, 568.

Fisher, J.R., Tully R.B. 1981 ApJS 47, 139.

Freedman, W.],., 1985 ApJ 299, 74

Freedman, W.L., 1988 ApJ 326, 691.

Freedman, W.L., 1990 ApJ 355, 1,35.

Freedman, W.],., Madore, B.F. 1990 ApJ 365, 186.

Freedman, W.L., *et al.* 1994a ApJ 427, 628.

Freedman, W.L., *et* al. 1994b Nature 371, 757.

Garcia, A. M., 1993 A&ASupp 100, 47.

Graham, J. A., *et al.* 1996 ApJ, in press.

hill, R., *et* d. 1996 ApJ, in press.

Hoaglin, 1).C, Mosteller, F. & Tukey, J .W. 1983 *Understanding Robust and* II;xf>lor-story *Data Analysis* (Wiley, New York).

Holtzman, J. A., *et al.* 1995a PASP 107, 156.

Holtzman, J. A., *et al.* 1995b PAS]' 107) 1065.

1 luchtmeier, W.K., Richter, O.-G. 1989 A *General Catalog of HI Observations of Galaxies* (New York: Springer).

Hughes, S.M.G. 1989 AJ 97, 1634.

Hughes, S.M.G. *et al.* 1994 ApJ 428, 143.

Hughes, S., Han, M., 11 OCSSCI, J. 1996, in Science with HST - 11, eds. 1'. Benvenuti, F.D. Macchetto, & E. J. Schreier (ESA/NASA Publication), p46.

Kelson, D.D. *et al.* 1990 ApJ 463, 26

Lafler, J., Kinman, (1'.1), 1965 ApJS 11, 216.

Lee, M.G., Freedman, W.L., Madore, B.F. 1993, ApJ 417, 553.

Madore, B.F., Freedman W.L. 1991 PASP 103, 933.

Madore, B.F. 1982 ApJ 253, 575.

MZI(1OJC, B.F., *et al.* 1996, in preparation.

Marcelin, M., Petrosian, A.R., Amram, 1'., Boulesteix, J. 1994 A&A 282, 363.

Mould, J., Sakai, S., Hughes, S., Han, M. 1996 Proceedings of the STScI May Symposium on the Extragalactic Distance Scale (Cambridge University Press), in press.

Oey, M. S., Kennicutt, R.C. 1993 ApJ 411, 137.

Pierce, M.J. Tully, R.B. 1992 ApJ 387, 47.

Prada, F. *et al.* 1996, private communication.

Rawson, D. M., *et* al. 1996 ApJ, submitted.

Rubin, V.C., Burbidge, E.M., Burbidge, G.R., Crampin, D. J., Prendergast, 1{.11. 1965 ApJ 141, 759.

Saha, A., Hoessel, J.G. 1990 A,] 99, 97.

Saha, A., *et al.* 1994 ApJ 425, 14.

Saha, A., *et al.* 1996 ApJ submitted.

Sandage, A., Bedke, J. 1985 AJ 90, 1992.

Schechter, P.L., Make, M., Saha, A. 1993 PASP 105, 1342.

Schmidt 1).1'., *et al.* 1994 ApJ 432, 42.

Silbermann, N. A., *et al.* 1996 ApJ, in press.

Stellingwerf, R.F. 1978 ApJ 224, 953.

Stetson, P.B. 1994 I'AS]' 106, 250.

Tanvir, N.R., *et* al. 1995 Nature 377, 27.

Tanvir, N.R. 1996 Proceedings of the STScI May Symposium 011 the Extragalactic Distance Scale, (Cambridge University Press), in press.

Tonry, J.],., Blakeslee, J.] '., Ajhar, E.A., Dressler, A. 1996 Sissa preprint 9609113.

Tormen, G., Burstein, D. 1995 ApJS 96, 123.

Tully, R.B. 1988 *Nearby Galaxies Catalog*, (Cambridge: Cambridge University Press).

Walker, A. IL. 1994 PASP 106, 828.

Welch, D.L., Stetson, P.B. 1993 AJ 105, 1813.

Willick, J.A. *et al.* 1996 ApJ 457, 460.

'Piris preprint was prepared with the AAS LaTeX macros v4.0.

Table 1. Epochs of Observations.

Epoch	Julian Date	Filename	Date	Exposure times	Filter
1	49521.832	u2781q01t	18/06/94	1200.() 1600.()"	F555W
2	49530.612	u2781r01t	27/06/94	1 200.() 1600.0"	F555W
3	49543.952	u2781t01t	10/07/94	1200.() 1600.()"	F555W
4	49545.762	u2781u01t	12/07/94	1200.0 1600.0	F555W
5	49549.586	u2781v01t	16/07/94	1200.0 1600.()	F555W
6	49552.806	u2781w01t	19/07/94	1200.0 1600.0	F555W
7	49557.044	u2781x02t	24/07/94	1200.() . .	F555W
8	49561.927	u2781y01t	28/07/94	1200.0" 1600.()	F555W
9	49573.584	u2781s01t	9/08/94	1200.0 1600.0	F555W
10	49573.861	u2782001t	9/08/94	1200.0 1600.0	F555W
11	49581.226	u2782101t	17/08/94	1200.() 1600.0	F555W
12	49887.615	u2o30101t	19/06/95	1200.0 1600.0	F555W
13	49902.628	u2o30201t	4/07/95	1200.0 1600.0	F555W
14	49921.593	u2o30301t	23/07/95	1200.() 1600.0	F555W
15	49946.395	u2o30401t	17/08/95	1200.0" 1600.0	F555W
1	49521.966	u2781q03t	18/06/94	1200.0 1600.0	F814W
2	49530.746	u2781r03t	27/06/94	1200.0 1600.()	F814W
8	49567.754	u2781z06t	3/08/94	1200.() .. .	F814W
12	49887.631	u2o30103t	19/06/95	1200.()" 1600.()	F814W
.	49902.645	u2o30203t	4/07/9[)	260.() 260.0	F555W
...	49902.650	u2o30204t	4/07/95	260.() 260.0	F814W

Table 2. Reference Star Photometry.

ID	Chip	RA	(,12000)	Dec	X	Y	V_{Alf}	I_{Alf}	$V_{D\ oph}$	$I_{D oph}$
R 1	1	22:37: 1.47	34:28	:10.6	206.2	100.1	24.15 ± 0.08	23.81 ± 0.23	24.43,1 0.09	23.62:1 ().61
R 2	1	22:37: 0.40	34:28:	9.4	211.7	394.2	21.91 ± 0.03	20.24 ± ().()4	22.06 ± 0.08	20.05 ± 0.38
R 3	1	22:36:59.90	34:28:	1.0	385.4	544.3	24.67:1 0.07	24.344 0.19	24.744 ().07	24.32 ± ().97
R 4	1	22:36:59.69	34:28:	4.6	301.9	595.6	25.474 0.09	22.34 ± 0.12	25.53 ± 0.06	22.384 0.53
1{ 5	2	22:36:59.28	34:28	:23.4	334.6	102.8	23.35,1 0.04	22.364 0.04	23.41:1 0.07	22.57:1 ().27
R 6	2	22:36:59.05	34:28	:31.8	356.()	190.0	24.36,1 0.06	24.07 ± 0.13	24.47,1 0.09	24.44:1 0.37
R 7	2	22:36:56.71	34:28	:31.9	648.0	214.9	22.014 0.02	10.743 (),03	22.12 ± 0.10	19.85 ± ().15
R 8	2	22:36:58.07	34:28	:56.4	457.9	448.6	23.38 ± ().()6	21 .12 ± ().02	23.45 ± 0.08	21.24,1 0.05
R 9	2	22:36:57.52	34:28	:56.0	525.8	450.4	25.014 ().()6	23.504 0.06	25.03 ± ().10	23.50 ± 0.07
R 10	2	22:36	:58.05	34:28:58.9	458.1	473.5	20.47,1 0.07	19.68 ± ().()1	20,604 0,08	19.80 ± 0.07
R 11	2	22:36:57.94	34:29:	5.9	465.7	545.4	25.06 ± ().()8	24.92: 0.36	25.14 ± ().()7	24.85 ± ().2()
R 12	3	22:37: 2.11	34:28:27.5		121.6	117.1	25.41 ± 0.08	24.96 ± 0.13	25.51,1 0.04	25.074 0.19
R 13	3	22:37: 1.90	34:29:12.9		582.4	127.2	23.494 0.06	22.73 ± 0.39	23.58 ± 0.04	22.95 ± ().10
R 14	3	22:37: 2.37	34:29:13.5		583.3	185.9	24.62 ± 0.07	24.40 ± 0.17	24.78 ± 0.05	24.37:1 0.10
R 15	3	22:37: 2.48	34:29: 3.8		484.5	192.9	24.76 ± 0.08	23.77 ± ().()7	24.83 ± 0.04	23.76:1 0.06
R 16	3	22:37: 2.84	34:28:22.6		64.2	204.1	25.05,1 0.09	24.243 ().12	25.23,1 0,08	24.264 0.04
R 17	3	22:37: 3.06	34:28:36.1		200.()	243.1	24.39 ± 0.07	23.974 0.59	24.48 ± 0.04	24.314 ().()7
R 18	3	22:37: 4.91	34:28:40.0		220.8	476.8	25.704 0,09	25.30 ± 0.23	25.95 ± 0.09	25.274 0.15
R 19	3	22:37:5.04	34:28:50.5		325.4	500.8	25.55 ± 0.10	24.75 ± ().17	25.79 ± 0.05	24.89 ± 0.11
R 20	3	22:37: 5.45	34:28	:51.0	326.9	552.6	24.264 0.08	21.'.294 ().09	24.30:4 0.06	21.36 ± 0.08
R 21	3	22:37: 5.57	34:28:49.7		312.6	567.1	25.42 ± 0.07	22.713 0.15	25.464 0.05	22.88,1 0.07
R 22	3	22:37: 5.97	34:29:15.4		567.3	637.6	23.624 0.08	20.714 0.05	23.824 0.04	20.814 0.05
R 23	3	22:37: 6.12	34:29: 2.0		430.4	645.0	23.30:1 0.06	20.97:1 0.03	23.38 ± 0.03	21.044 0.04
R 24	3	22:37: 6.41	34:28:50.3		310.()	672.1	25.273 0.08	22.19 ± ().04	25.354 0.06	22.27,1 ().()5
R 25	3	22:37:6.45	34:29:13.6		545.3	695.1	24.95 ± ().08	22.27 ± 0.04	25.05 ± 0.03	22.30:1 0.07
R 26	3	22:37: 6.81	34:29: 4.9		453.5	734.0	24.52 ± 0.08	23.98 ± ().17	25.054 0.09	24.353 ().()7
R 27	4	22:37: 3.77	34:28:13.8		311.6	109.2	**2404,1** 0.08	23.93,1 ().61	25.12 ± 0.09	24.203 0.16
R 28	4	22:37: 3.45	34:28	:11.6	271.2	128.6	24.93:1 0.06	24.82 ± (),17	24.97 ± 0.10	24.78 ± ().12
R 29	4	22:37: 2.85	34:28:	3.3	189.8	207.1	24.694 0.06	24.46 ± ().1()	24,71:1 0.07	24.37,1 0.10
R 30	4	22:37: 3.66	34:27:60.0		288.5	248.4	24.994 0.08	24.[]33 ().1()	**2[),()()** ±0.06	24.48 ± ().12
R 31	4	22:37: 4.11	34:27:50.9		339.3	343.2	21.23,1 0.09	19.64 ± 0.02	21.22 ± 0.03	19.70,1 ().07
R 32	4	22:37: 5.62	34:27:50.7		526.8	358.9	24.59:1 ().07	24.18,1 0,10	24,51:1 0.07	24.09:1 0.06
R 33	4	22:37: 5.09	34:27:48.6		459.0	374.7	24.58 ± 0.06	24.1 () ±0.20	24.60:1 0.06	24.14 ± ().17
R 34	4	22:37: 5.59	34:27:40.4		515.9	462.1	24.62,1 ().07	23.95: 0,48	24.644 0.06	24.25 ± 0.08
R 35	4	22:37: 5.21	34:27:33.8		463.8	525.6	24.014 ().08	23,59,1 0.53	24.02 ± ().()4	23.84 ± (). 13
R 36	4	22:37: 3.26	34:27:23.1		213.0	616.7	24.06,1 0.08	23.19 ± 0.12	24.014 ().()7	23.13 ± 0.14

Table 3. DoPHOT - ALLFRAME Comparison.

Chip	N	$\Delta F555W_{0.5}$	$\Delta F814W_{0.5}$
1	4	0.135,1 0.039	-0.0884 0,041
2	7	0.084 ±1 0.010	0.123,1 0.037
3	1 5	0.150 ±1 0.023	0.111:1 0.022
4	10	0.015,1 0.016	0.0564 0.034

'1'able 4. Calibrated DoPHOT magnitudes of Cepheids with good lightcurves.

Epoch		Single epoch magnitudes				
		V 1	V 2	V 3	V 4	V 5
V	1	26.00 ± 0.16	25.77 ± 0.13	27.20 + 0.24	25.36 ± 0.12	25.93:1 ().14
	2	24.91 ± 0.12	26.444 0.15	27.08 ± 0.23	26.20 ± 0.15	26.60,1 0.20
	3	25.43 ± 0.13	25.90 ± 0.13	26.48 ± 0.16	25.57 ± 0.12	26.084 0.15
	4	25.27,1 0.13	26.15 ± 0.14	26.52 ± 0.15	25.71,1 0.14	25.25 ± 0.13
	5	25.56 ± 0.16	26.55:1 0.18	27.37 ± ().32	26.05 ± 0.16	25.624 0.13
	6	25.77 ± 0.14	26.26 ± 0.14	27.32:1 0.26	26.29 ± 0.17	25.79,1 ().14
	7	26.19 ± 0.25	25.72 ± ().14	26.67,1 0.21	26.614 0.24	26.37,1 0.23
	8	26.29,1 0.14	25.51 ± 0.16	26.71:1 0.21	26.86 ± 0.20	26.3340.17
	9	25.10 ± 0.12	26.614 0.18	26.444 0.20	26.20 ± 0.14	26.25 ± 0.15
	10	25.05,{ 0.11	26.18 ± 0.17	26.69 ± 0.19	26.16 ± 0.15	26.414 0.16
	11	25.45 ± 0.12	25.314 0.13	27.32 ± 0.28	26.58 ± 0.18	25.59 ± ().13
	12	25.444 0.17	25.944 0.15	27,394 0.29	25.90 ± 0.13	25.46,10.12
	13	26.14 ± 0.17	25.544 0.14	27.50 ± 0,35	26.77 ± 0.19	26.244 0.16
	14	25.49 ± 0.15	25.1130.12	26.743 0.23	26.813 0,18	25.66 ± 0.14
	15	26.284 0.19	25.50 ± 0.13	26.36 ± 0.16	26.544 0.19	
1	1	24.92 ± 0.16	25.17 ± 0.16	26.334 0.28	24.85 ± 0.13	24.6740.13
	?	24.43 ± 0.15	25.66 ± 0.18	25.75,1 0.20	25.343 0.18	24.97 ± 0.14
	7	24.08 ± 0.13	25.26 ± 0.17	26.20 ± 0.34	24.7140.13	25.0340.19
	12	24.734 0.21	24.844 0.14	26,514 ().41	24.80,1 0.13	24.39,1 0.12
		V 6	V 7	V 8	V 9	V 10
V	1	25.95 ± 0.16	25.68 ± 0.09	27.93 ± 0.46	25.934 0.10	26.7530.21
	2	26.573 0.20	25.844 0.11	27.21,1 0.22	26.52 ± 0.19	26.59,10,21
	3	25.354 0.14	26.094 0.12	28,214 0.37	26.60 ± 0.17	26.1140.17
	4	25.49,1 0.15	26.16 ± 0.13	28.18 ± ().50	26.03 ± 0.10	26.6730.20
	5	25.76 ± 0.16	26.15 ± 0.13	27,24:1 0.26	26.03 ± 0.11	27.224 0.26
	6	25.68 ± 0,13	26.12 ± 0.13	26.89,1 ().18	26.26 ± 0.12	27.15 ± ().28
	7	26.65 ± 0.26	25.61,1 0.10	28.60 ± 1.13	26.49 ± 0.19	26.74,1 0.23
	8	26.66 ± 0.20	25.584 ().08	27.334 ().24	27.05 ± 0.29	27.95 ± 0.48
	9	25.314 0.15	25.91,10.12	26.93:1 0.21	26.1340.11	27.59 ± 0.40
	10	25.43 ± 0.15	25.89 ± 0.11	26.48 ± ().14	26.19,! 0.14	27.56 ± 0.44
	11	25.58 ± 0.15	26.40 ± 0.17	28.414 0.66	26.58 ± ().16	27.46 ± 0.35
	12	26.32 ± ().20	25.71:1 0.10	26.81,1 ().20	25.91 ± 0.11	2.7.43,1 0.41
	13	25.94 ± 0.18	26.39,1 0.15	28.28 ± 0.57	26.55 ± ().1 8	26.744 0.23
	14	26.924 0.61	25.51:1 0.08	27.30:1 ().23	26.58 ± 0.17	27.43,10.37
	15	26.53 ± 0.18	26.06:1 ().12	27.69:1 ().41	26.45 ± ().17	28.23:1 0.62
1	1	25,29,1 0.21	24.49 ± ().()8	26.70,1 ().41	24.71 ± 0.10	25.70 ± ().23
	2	25,15,1 0.17	24.77:1 0.09	26.06:1 0.22	25.07 ± ().1 2	25.45,1 ().'23
	7	25,504 ().26	24.56,1 ().14	20.37,1 ().4'2	24.88 ± 0.12	25.98,1 ().36
	12	25.29 ± ().21	24.56 ± 0.09	25.68 ± ().18	24,62,1 0.09	26.80 ± 0.63

'J'able 4-Continued

Epoch		Single epochmagnitudes			
		v]]	V 12	V 13	V]4
V	1	25.713 0.15	26.29:1 0.20	27.713 0.71	25.933 0.16
	2	'2(3.40,1 0.18	25.394 0.14	27.34:1 0.43	26.66 ± 0.26
	3	26.0230,18	25.914 0.17	28.56 ± 1.10	25.36 ± 0.13
	4	26.0140.17	25.944 0.18	27.093 0.34	25.40 ± 0.13
	5	26.25 ± 0.18	26.08:1 0.20	27.073 0.35	25.53 ± 0.13
	6	26.42 ± 0.29	25.56 ± 0.16	27.734 0.48	25.96 ± 0.16
	7	26.404 0.23	25.39 ± 0.15	,··	25.90 ± 0.21
	8	26.054 0.15	25.513 0.14	27.12 ± 0.39	26.10 ± 0.17
	9	26.8740.26	26.15:10.21	28.624 1.02	26.41:1 0.21
	10	26.55 ± 0.22	26.093 0.22	28.294 0.89	26.28 ± 0.22
	11	25.79 ± 0.14	25.31,10.13	27.43 ± 0,43	**25.60:10,13**
	12	26.29 ± 0.17	25.79 ± 0.17	28.984 1.62	25.86 ± 0.14
	13	25.89 ± 0.15	25.554 0.16	···	26.084 0.20
	14	25.814 0.14	26.124 0.22	27.72 ± 0.52	25.51:1 0.14
	15	26.204 0.23	25.86 ± 0.25	28.44 ± 0.66	26.60 ± 0.21
1	1	24.96 ± 0.17	25.10,1 ().18	26.08 ± 0.40	24.98 ± 0.20
	2	25.48 ± 0.23	24.414 ().14	26.65,1 0.60	25.06 ± 0.17
	7	25.15 ± 0.21	24.94:1 ().20	27.014 1.03	25.08 ± 0.23
	12	25.18 ± 0.20	24.75 ± 0.17	26.32,1 0.43	24.68 ± 0.17

'J'able **5.** Calibrated ALLFRAME magnitudes of Cepheids with good lightcurves.

Epoch		Single epoch magnitudes				
		V 1	V 2	V 3	V 4	V 5
V	]	26.01 ± 0.26	25.57,1 0.13	27.21< 0.28	25. 55 ± 0.19	25.87,4 ().14
	2	24.91 ± 0.11	26.04 ± 0.18	26,643 0.23	26.13,1 0.13	26.33 ± 0.17
	3	24.97,1 0.09	26.17 ± 0.19	···	26.12 ± ().21	26.28 ± ().14
	4	25.36 ± 0.12	···	26.57:1 0.20	25.46 ± 0.13	26.144 ().21
	5	···	25.754 0.16	26.574 0.23	25.60 ± ().13	25.46 ± 0.17
	6	···	26.35:1 0.25	27.17,1 0.35	26.00 ± ().16	25.69 ± ().1()
	7	25.45 ± 0.89	26.07:1 0.20	27.36 ± 0.30	26.22 ± 0.16	25.98 ± ().19
	8	25.84 ± 0,33	25.57 ± 0.19	26.46 ± 0.19	26.344 0.31	26.1140.25
	9	25.98 ± 0.18	25.31:1 ().16	26.72 ± 0.21	26.94:1 0.25	26.19 ± 0.17
	10	24.99 ± ().13	25.904 0.47	26.60 ± 0.22	26.17 ± 0.16	26.4730.19
	11	25.25,1 0.13	25.11:1 0.20	27.28,1 ().27	26.50 ± 0.18	25.654 0.12
	12	25.21 ± 0.13	25.8040.11	27.75 ± 0,43	25.8840.15	25.46 ± 0.13
	13	26.06 ± 0.15	25.354 0.12	27.55 ± 0.48	26.92 ± 0.22	26.36 ± 0.16
	14	24.98 ± ().12	25.15 ± 0.13	26.684 0.20	26.81:1 0.32	25.56 ± 0.21
	15	26.07 ± 0.18	25.59 ± 0.16	26.393 0.15	26.43,1 0.26	2G.934 0.29
I	1	24.82 ± 0.14	25.03 ± 0.14	26.17 ± 0.22	24.82 ± 0.12	24.G34 0.07
	2	24.15 ± O.(N	25.40 ± 0.16	25.65 ± 0.19	25.15 ± ().10	24.96 ± 0.10
	9	23.99 ± 0.12	25.094 0.24	26.26 ± 0.38	24.7240.13	25.324 0.23
	12	24.29 ± 0.15	25.034 0.12	26.63 ± 0.36	25.00 ± ().13	24.774 0.10
		V 6	V 7	V 8	V 9	V lo
V	1	25.46 ± ().13	25.62 ± 0.12	28.02,1 '0.58	25.93 ± 0.12	26.94 ± 0.31
	2	25.91 ± ().24	25.93 ± 0.18	27.344 0.37	26.50 ± 0.38	26.74 ± 0.32
	3	24.88 ± 0.11	25.82 ± 0.17	26.47 ± 1.13	25.91:1 ().15	27.65 ± 0.51
	4	24.994 0.11	26.20 ± 0.18	27.49 ± 0.43	25.84,1 ().22	26.554 ().34
	5	25.01 ± 0.12	26.10 ± 0.16	28.31,1 ().74	26.00 ± 0.12	26.72 ± 0.27
	6	25.36 ± 0.13	26.064 0.13	27.34:1 0.37	25.97 ± 0.16	27.334 0.45
	7	25.49,1 0.14	26.064 ().15	26.974 0.24	26.34 ± 0.18	27.24,1 0.34
	8	25.98 ± ().24	25.50 ± 0.19	···	26.38 ± 0.26	26.64 ± 0.25
	9	25.90,1 0.32	25.61,1 0.11	27.30,1 0,34	26.93 ± ().35	27.57'4 0.40
	10	24.96 ± 0.11	25.92 ± 0.10	26.55 ± 0.22	26.19 ± ().22	27. 62 ± 0.51
	11	25.36 ± 0.14	26.214 0.24	28.03,1 0.59	26.39 ± ().19	27.19 ± ().34
	12	2G.244 0.23	25.72 ± ().13	26.93 ± 0,23	25.844 0.14	27.45:1 0.36
	13	25.49 ± ().15	2G.503 0.22	27.96 ± 0.77	26.52 ± 0.19	2G.824 0.22
	14	24.90 ± 0.11	25.58 ± 0.13	27.57:1 0.30	26.45:1 0,23	27.36 ± ().38
	15	26,35,1 0.21	26.13,1 ().17	27.80,1 ().5()	26.60 ± 0.26	28.20 ± 0.86
I	1	24.53,1 ().1()	24.64 ± ().1 G	26.82 ± ().44	24.83 ± (),15	25.71,1 0.19
	2	24.89 ± ().13	24.81,1 ().1(;	26.15 ± 0.34	25.04 ± (). I 3	25.62 ± ().22
	9	25.12,1 0.22	24.643 0.17	26.66 ± 0.44	24.97 ± ().2.1	26.02,1 0.33
	12	25.12,1 0.13	24.80:1 0.1:)	26.01 ± 0. 25	24,77,1 0.11	26.89 ± ().72

Table 5- Continued

Epoch		Single epoch magnitudes			
		V 11	V 12	V 13	V 14
\/	1	25.90 ± 0.19	26.244 0.25	28.51,1 1.68	26.17 ± 0.32
	2	26.604 0.22	25.27,! 0.10	27.214 0.66	26.73 ± 0.25
	3	26.943 0.41	26.004 0.21	28.104 ().74	26.48 ± 0.17
	4	26.15 ± ().32	25.92,1 0.18	26.08,1 0.96	25.35 ± 0.14
	5	26.064 0.16	25.90 ± 0.16	25.38 ± 0.54	25.41:1 0.20
	6	26.233 0.24	25.92 ± 0.17	27.17 ± 0.47	25.55,1 0.13
	7	26.604 0.24	25.50 ± 0.15	27.50 ± 1.10	25.80,1 0.14
	8	26.63 ± 0.38	25.30 ± 0.16	...	25.93,1 0.33
	9	25.84,1 0.19	25.52,1 0.23	25.24 ± 0.64	26.18 ± 0.17
	10	26.73 ± 0.25	26.04:1 0.26	27.74:1 0.60	26.404 0.17
	11	25.79 ± 0.15	25.144 0.15	27.314 ().45	25.59 ± 0.16
	12	26.424 0.23	25.99 ± 0.30	28.774 2.06	26.00 ± 0.19
	13	26.16 ± 0.20	25.47 ± 0.17	28.43,1 1.24	26.344 0.25
	14	25.83 ± 0.13	26.19 ± ().18	27.794 0.60	25.60 ± 0.15
	15	26.40 ± 0.23	26.16 ± 0.22	28.03 ± 1.00	26.51,1 0.31
1	1	25.13 ± ().15	25.32,1 0.16	26.15 ± 0.44	25.16 ± ().17
	1	25.63,1 0.29	24.56 ± 0.10	27.10 ± 0.77	25.16 ± 0.14
	2	25.323 0.22	24.95,1 0.20	26.92,1 1.62	24.944 0.24
	2	25.52,1 0.24	24.96 ± 0.14	27.754 1.86	24.89 ± 0.15

Table 6. Cepheids with good lightcurves.

ID	Chip	R A (J2000)	Dec	X	Y	P_{Alf}	$<V>_{Alf}$	$<V-I>_{Alf}$	P_{Doph}	$<V>_{Doph}$
V1	2	22:36:59.60	34:28 :21,0	296.3	75.1	42.59	25.323 0.06	1.06: 0.09	42.18	25.51 ± 0.0
V2	2	22:36:56.53	34:28 :42.3	661.8	322.1	21.19	25.63 ± 0.06	0.544 0.10	21.35	25.79 ± 0.0
V 3	2	22:36:58.30	34:28 :45.9	437.8	340.7	13.91	26.844 0.08	0.8630.16	13.91	26.8340.0
V4	2	22:36:58.82	34:28 :47.4	372.4	350.4	22.60	26.084 0.05	1.09,1 0.08	22.60	26.12 ± 0.0
V 5	2	22:37:0.23	34:29:26.7	162.1	732.2	33.94	25.994 0.05	1.10 ± 0.08	33.87	25.874 0.0
V 6	2	22:36:59.92	34:29 :28.2	199.8	750.4	29.05	25.334 0.05	0.75 ± 0.08	29.43	25.86 + 0.0'
V 7	3	22:36:59.84	34:28 :22.6	265.1	88.9	39.90	25.88,1 0.04	1.09,1 0.09	39.72	25.894 0.0
V 8	3	22:36:59.00	34:28 :33.9	360.3	212,1	11.13	27.35 ± 0.13	1.06:1 0.23	11.16	27.36 ± 0.1
V 9	3	22:36:58.57	34:28 :38.7	410.6	265.2	24.41	26.18 ± 0.06	1.304 ().09	25.83	26.294 0.0
V 10	4	22:36:59.83	34:28 :29.9	261.1	163.3	11.61	27.14 ± 0.11	1.16 ± 0.25	11,61	27.014 0.0
V 11	4	22:36:58.67	34:29: 9.7	371.8	575,5	19.82	26.193 ().06	0.82 ± 0.14	19.86	26.11 ± 0.0
V 12	4	22:36:58.67	34:29 :11.8	369.7	597.4	24.82	25.723 0.05	0,83,1 0.09	26.68	25.734 ().0
v 13[a]	4	22:36:58.43	34:29 :20.1	392.5	683.2	15.04	26.814 0.23	0.00 ± 0.56	14.99	27.664 0.2
V14	4	22:36:59.37	34:29 :30.5	266.6	779.3	41.20	25.894 0.05	1.05 ± 0.10	37.54	25.854 0.0

[a]Not used in 1'1, fits due to unusual $<V-I>_{Alf}$

Table 7. Fits 101'1, relations

Sample	N	DM(V)	DM(I)	$E(V - I)$)	DM_0
			DoPHOT		
All	14	31.43 ± 0.09	31.17 ± 0.07	0.26 ± 0.06	30.80 ± 0.10
Chip 2	G	31.28	31.16	0.12	30.98
Chip 3	3	31.64	31.13	0.51	30.40
Chip 4	5	31.48	31.22	0.26	30.84
1'> 15	10	31.33	31.12	0.21	30.82
1'>20	9	31.36	31.15	0.21	30.84
1'>25	7	31.45	31.20	0.24	30.85
			ALLFRAME		
All	13	31.30 ± 0.10	31.15 ± 0.07	0.16 ± 0.06	30.92 ± 0.09
Chip 2	G	31.15	31.08	0,07	30.98
Chip 3	3	31.58	31.24	0.34	30.75
Chip 4	4	31.34	31.18	0.15	30.96
P > 15	10	:31.25	31.13	0.11	30.97
1'> '20	9	31.25	31.13	0.12	30.95
1' > 25	5	31.40	31.28	0.13	31.09

Table 8. Error Budget in the NGC 7331 Distance.

Source of Uncertainty	Uncertainty(mag)	Uncertainty(mag)
a) WFPC2 F555W$_{0.5}$ to V zero point	±0.04	
b) WFPC2 F814W$_{0.5}$ to I zero point	±0.04	
[A] Zero points (1.45a+ 2.45b)[a]		±0.11
c) F555W$_{0.5}$ aperture correction	±0.04	
d) 1"814\V0.5 aperture correction	±0.05	
e) 1)01'110'1' PL fit	±0.10	
f) ALLFRAME PL fit	±0.09	
[B] DoPHOT DM (c + e)[a]		±0.11
[C] ALLFRAME DM (c + f)[a]		±0.10
[D] Metallicity		±0.02
[It] LMC Distance Modulus		±0.10
NGC 7331 DM (DoPHOT) (A+B+D+F)[a]		±0.19
NGC 7331 DM (ALLFRAME) (A+c+D+F)[a]		±0.18

[a]All sums are in quadrature.

'1'able 9. Distances to NGC 7331

Method	Distance (Mpc)	Reference
M31/NGC 7331 velocities	17.7	Rubin et al. 1965
M31/NGC 7331 diameters	15.4	Rubin et al. 1965
Tully-Fisher(H)	12.0	Aaronson et al. 1982
11[, = 75	14.3	Tully 1988
Tully-Fisher(B)	9.6	Bottinelli et al. 1985
Cepheids	15.3	This paper (ALLFRAME)

'J'able 10. ~ IRTF Calibration.

Galaxy	DM	logΔV	$H_{0.5}$	Source of Distance
NGC224 (M31)	24.40	2.742	*0.91*	Freedman & Madore 1990
NGC300	26.66	2.371	7.00	Freedman 1990
NGC598 (M33)	24.50	2.392	4.38	Freedman 1990
NGC925	29.84	2.422	8.74	Silbermann et al. 1996
NGC2403	27.50	2.488	6.45	Freedman 1990
NGC3031 (M81)	27.80	2.716	4.38	Freedman et al. 19!)4tJ
NGC3351 (M95)	30.01	2.573	7.41	Graham et al. 1996
NGC3368 (M96)	30.32	2.709	6.87	Tanvir et al. 1995
NGC3621	29.20	2.536	7.40	Rawson et al. 1996
NGC4536	31.10	2.576	8.30	Saha et al. 1996
NGC7331	30.92	2.740	6.44	This paper

Table 11. DoPHOT Aperture Correction Spatial Coefficients.

Chip	C0	C1	C2	C3	C4	C5
			F555W			
1	-1.00531	7.2229191 ¢-5	3.8262901>4	-7.7324231)-8	−4.587308E-7	−7.685230E-9
2	-0.754943	1.9419041(>4	3.6651 15E-4	- 3.0656321 ¢-7	-4.3451701>7	1.1432391':-7
3	-0.764054	2.5506441¢-5	3.4842961>4	- 7.6145711 ¢-8	- 4.4478921 ¢-7	1.3635071 ¢-7
4	- ().755136	2.384645E-4	4.2555721>4	- 3.2532831; 7	-6.0872601>7	7.9686571 <-8
			F814W			
1	0.987125	7.9066891'>5	1.4497311>4	- 2.1731951 }-7	- 2.5048041 t-7	2.7523831 ¢-7
2	- ().904758	1.835472E-4	2.9479961 ¢-4	- 2.8782371 ¢-7	-3.6485801>7	1.4342791 ¢-7
3	-0.862129	7.1244841	;-6 2.3734781>4	-1 .0447 99E-7	- 3.485253E-7	2.2858431¢-7
4	–0.908892	2.751 133E-4	3.4908401 ¢-4	- 2.6750651 ¢-7	- 3.724]36]>7	- 1,0419731 ¢-7

Table 12. Zero-points and Aperture Corrections.

Filter	Chip PC1	Chip WF2	Chip WF3	Chip WF4
	1)0} '110"1' Zero-])oillts			
F555W	-7.569	-7.549	-7.477	-7.572
F814W	-8.923	-8.341	-8.408	-8.432
	ALLFRAME Aperture Corrections			
F555W	- 0.057	- 0.037	- 0.026	-1 0.0)09
F814W	-0.072	-1 0.019	-1 0.006	-1 0.030
	ALLFRAME Zero-points			
F555W	.0967	- 0.958	· 0.950	. 0.973
F814W	- 1.861	-1.823	-1,842	-1.870

Figure Captions

Fig. 1.- A 10 x 10 arcmin image of NGC 7331, derived from BVR frames obtained with the Prime Focus TEK camera on the Isaac Newton Telescope. The position of the WFPC2 field is indicated by the chevron, and the position Of SN1959D is also marked. North is to the right, and East is up (for purely aesthetic reasons). The background galaxies to the north are (from west to east) NGC 7337, NGC 7335, and NGC 7336.

Fig. 2.- An F555W medianed image of the WFPC2 mosaic (with North to the right, East up). The positions of the Cepheids in Table ?? are marked by labeled circles.

Fig. 3.- Comparison of calibrated $F555W_{0.5}$ and $F814W_{0.5}$ photometry of all stars in common between the DoPHOT and ALLFRAME sets of lightcurves, for each of the WFPC2 chips. The dashed line is the mean difference, of the points plotted, arid the solid line is the mean difference of the low rms isolated stars, chosen as reference stars in Table ??.

Fig. 4.- Finding charts for each Cepheid listed in Table ??. Each chart is centered on the Cepheid, and is 4 x4 arcsec squared (i.e. 40X40" WF pixels). North is up, east to the left.

Fig. 5.- Light curves, phased to the relevant period, for each Cepheid listed in Table ??. On the left are the calibrated DoPHOT mags, on the right are the calibrated ALLFRAME mags.

Fig. 6.- I vs b' $-I$ color-magnitude diagram for all chips. For clarity, only every 10th star is plotted. Also shown are the Cepheids from Table ?? (open circles), including those outside the instability strip (open squares) that are not used in the 1'1, fits.

Fig. 7.- The solid curve is the V luminosity function for all stars with V - 1 <0.3 (ALLFRAME mags), representing the blue plume. The dashed line is a least squares fit, to this luminosity function between $V = 23$ and $V = 26$ mag. The dotted curve is the V luminosity function for all stars with $0.5 < V - I < 1.5$ (ALLFRAME mags).

Fig. 8.- V (upper panel) and I (lower panel) PL relations for the Cepheids listed in Table ?? (calibrated ALLFRAME mags). The NGC 7331 Cepheids are the solid circles, and the LMC Cepheids are the open circles. The straight lines are least squares fits with fixed slope (see text). '11' is the blue ($V - 1 = 0.0$) NGC 7331 Cepheid, which was excluded from the fits.

Fig. 9.- V (upper panel) and 1 (lower panel) PL relations for the Cepheids listed in '1'able ?? (calibrated 1)01'11[)'1'mags).

Fig. lo. - IRTF absolute calibration, with absolute $H_{-0.5}$ mags vs log(ΔV) - 2.5, from data in Table ??. Filled circles are the data used by Freedman (1990), filled squares are the galaxies with recent HST-derived Cepheid distances, and the filled star is NGC 7331. The dotted line is the Freedman (1990) calibration , the dashed line is a least squares fit solution 1,0 the Freedman (1990) set, of galaxies, the dashed-dotted line is a least squares fit solution to all but NGC 7331, and the solid line is the least squares solution including NGC 7331

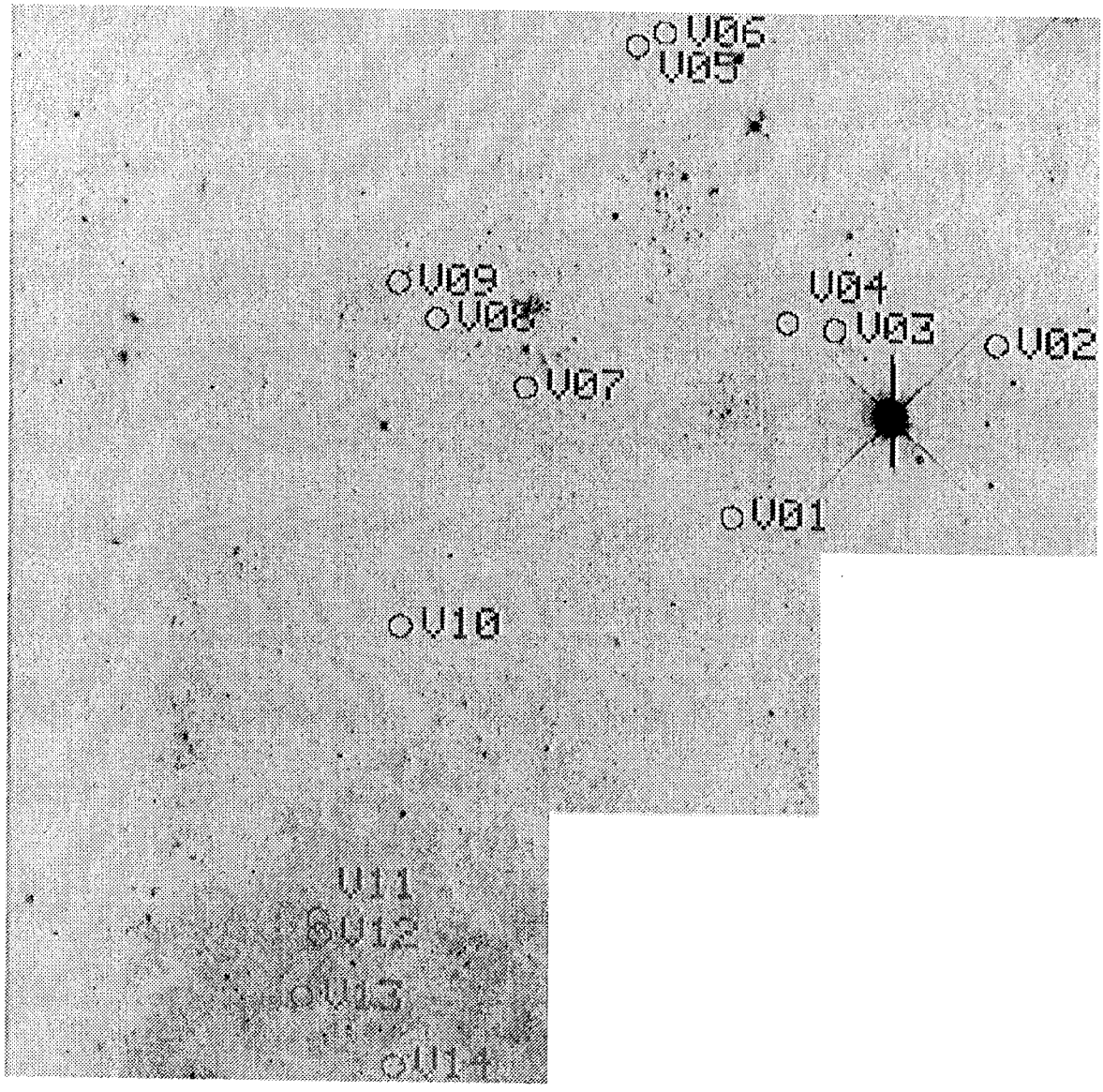
V06
V05
V09
V08
V04
V03
V02
V07
V01
V10
V11
V12
V13
V14

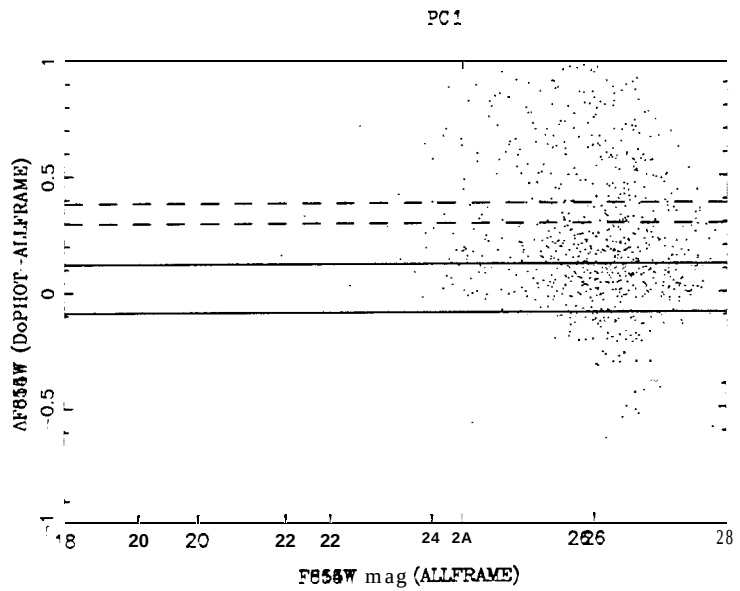
PC1
ΔF855W (DoPHOT−ALLFRAME)
F855W mag (ALLFRAME)

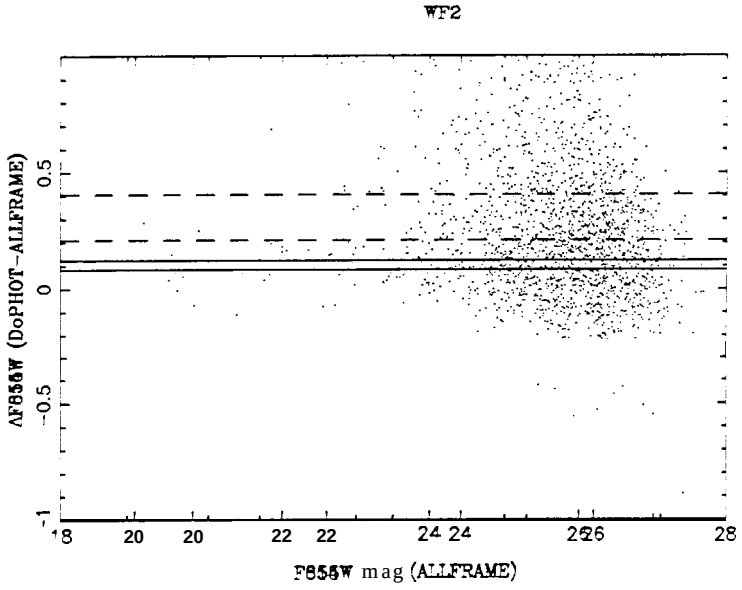
WF2
ΔF855W (DoPHOT−ALLFRAME)
F855W mag (ALLFRAME)

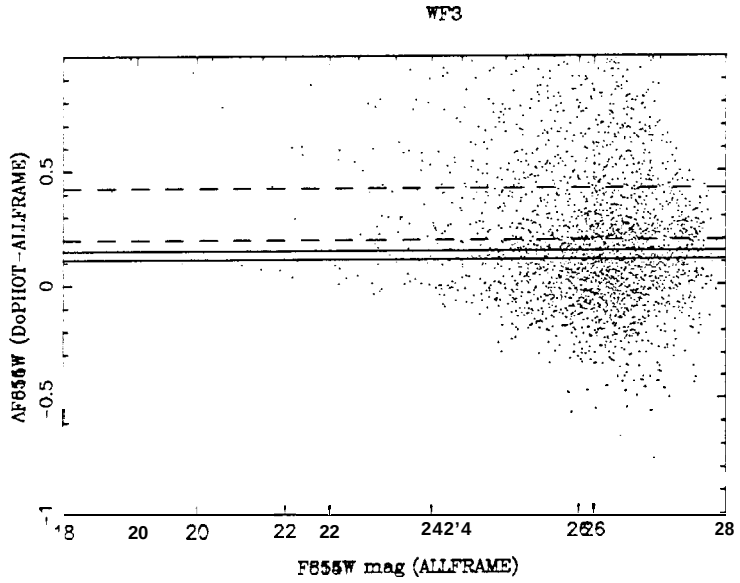
WF3
ΔF855W (DoPHOT−ALLFRAME)
F855W mag (ALLFRAME)

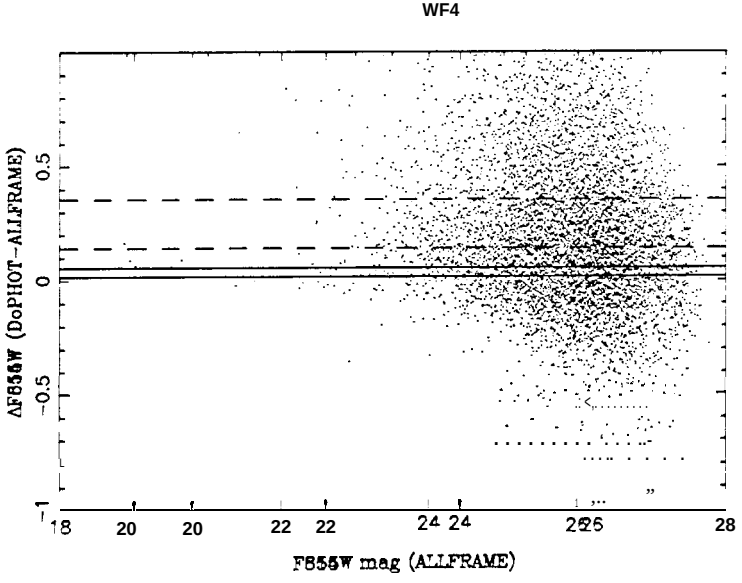
WF4
ΔF855W (DoPHOT−ALLFRAME)
F855W mag (ALLFRAME)

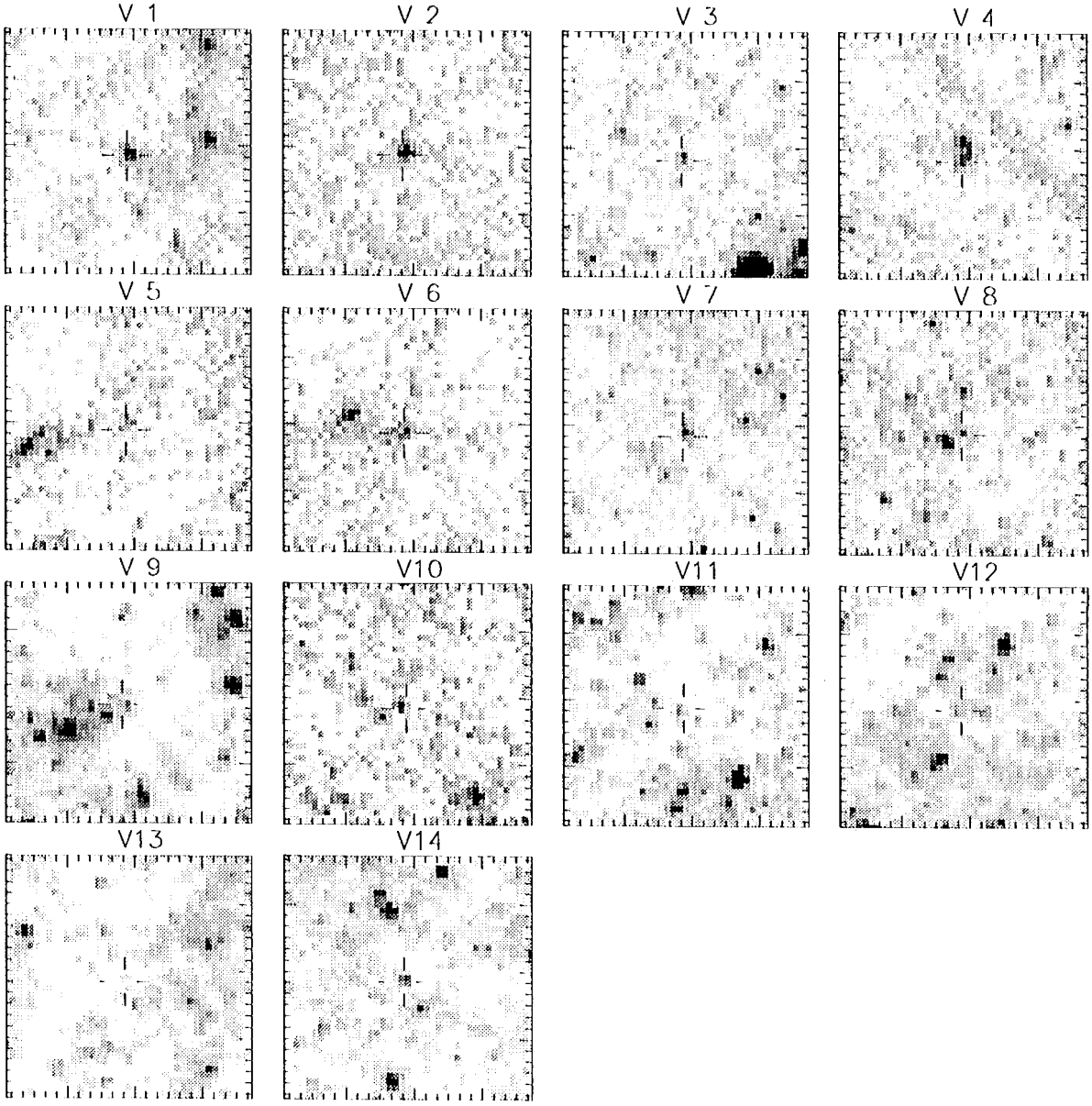
V 1
V 2
V 3
V 4
V 5
V 6
V 7
V 8
V 9
V10
V11
V12
V13
V14

NGC 7331

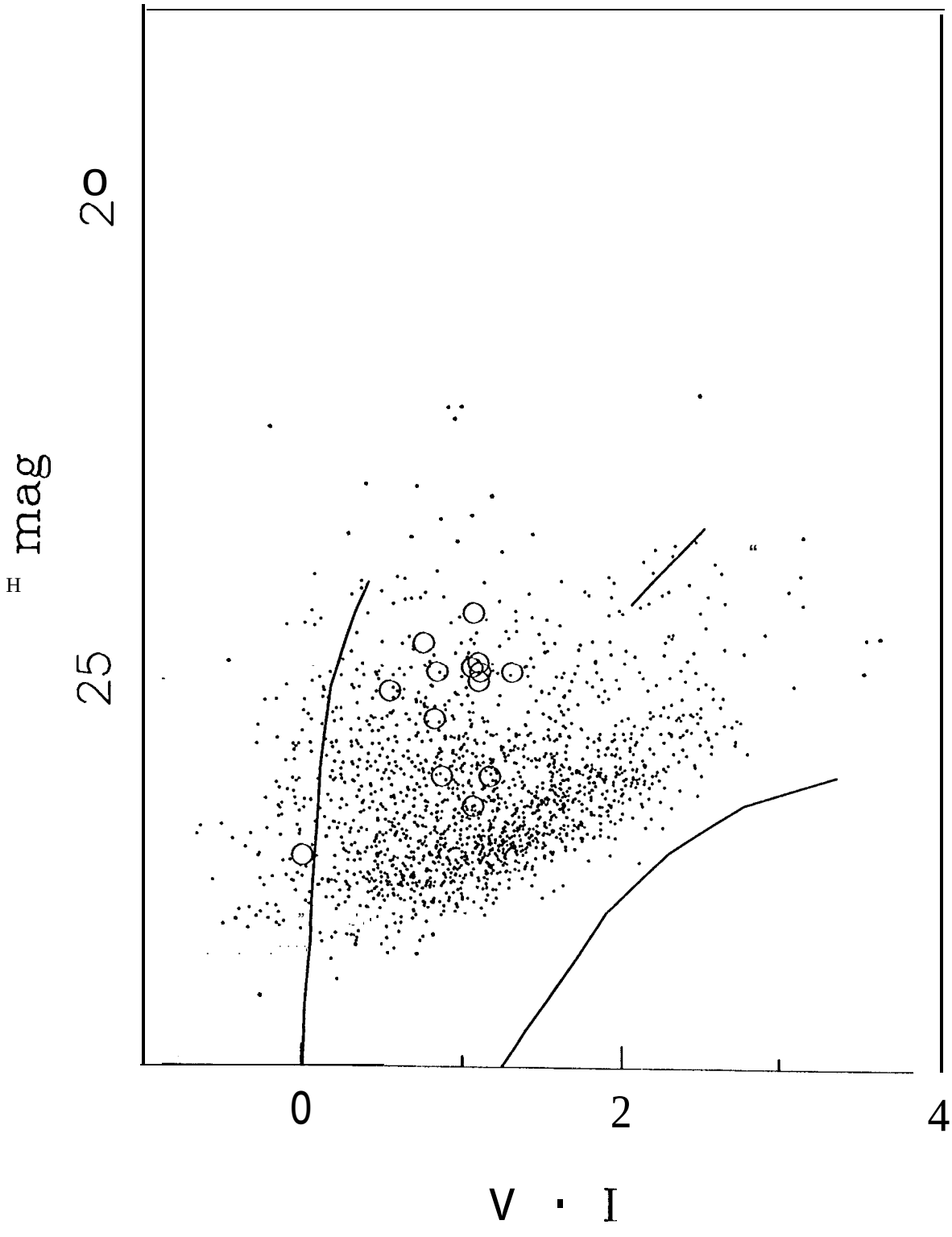

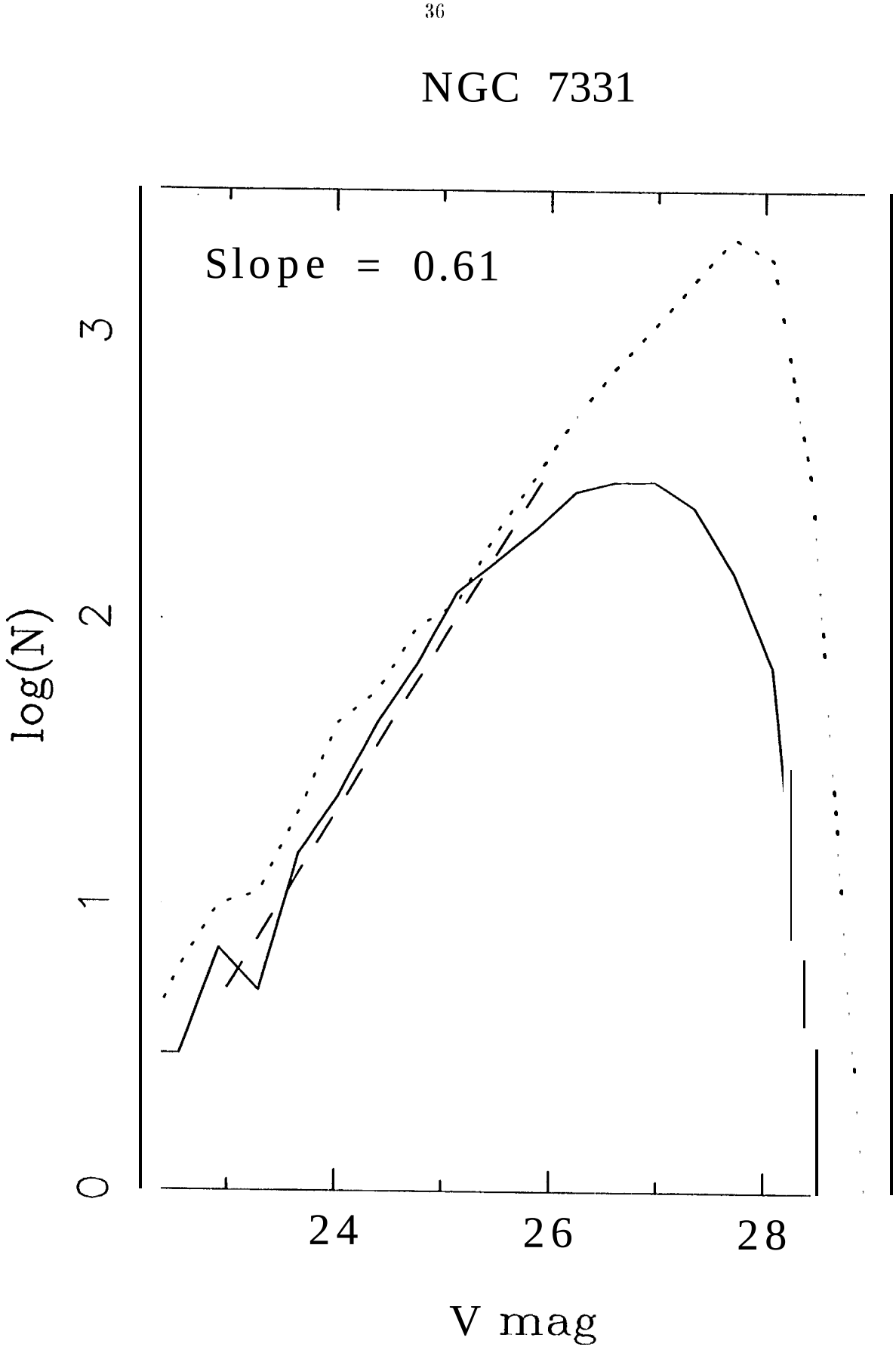
NGC 7331
Slope = 0.61
log(N)
0
1
2
3
24
26
28
V mag

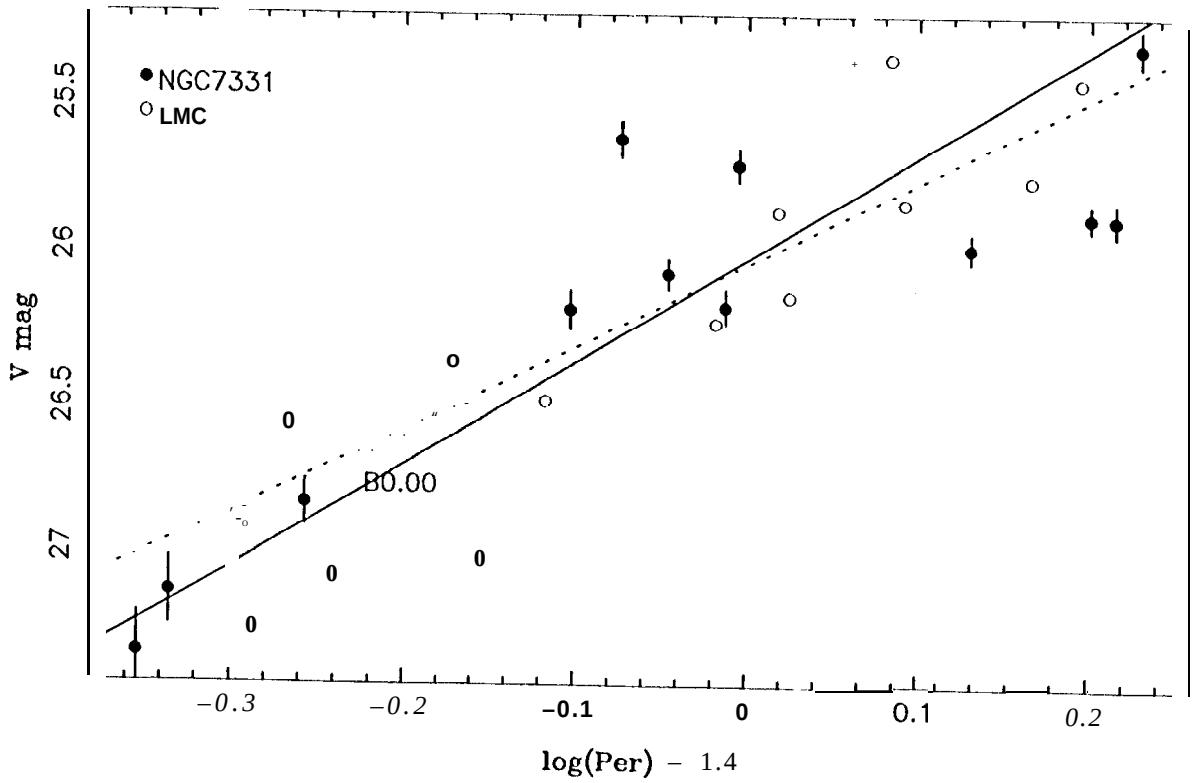
NGC7331
LMC
V mag
25.5
26
26.5
27
B0.00
−0.3
−0.2
−0.1
0
0.1
0.2
log(Per) − 1.4

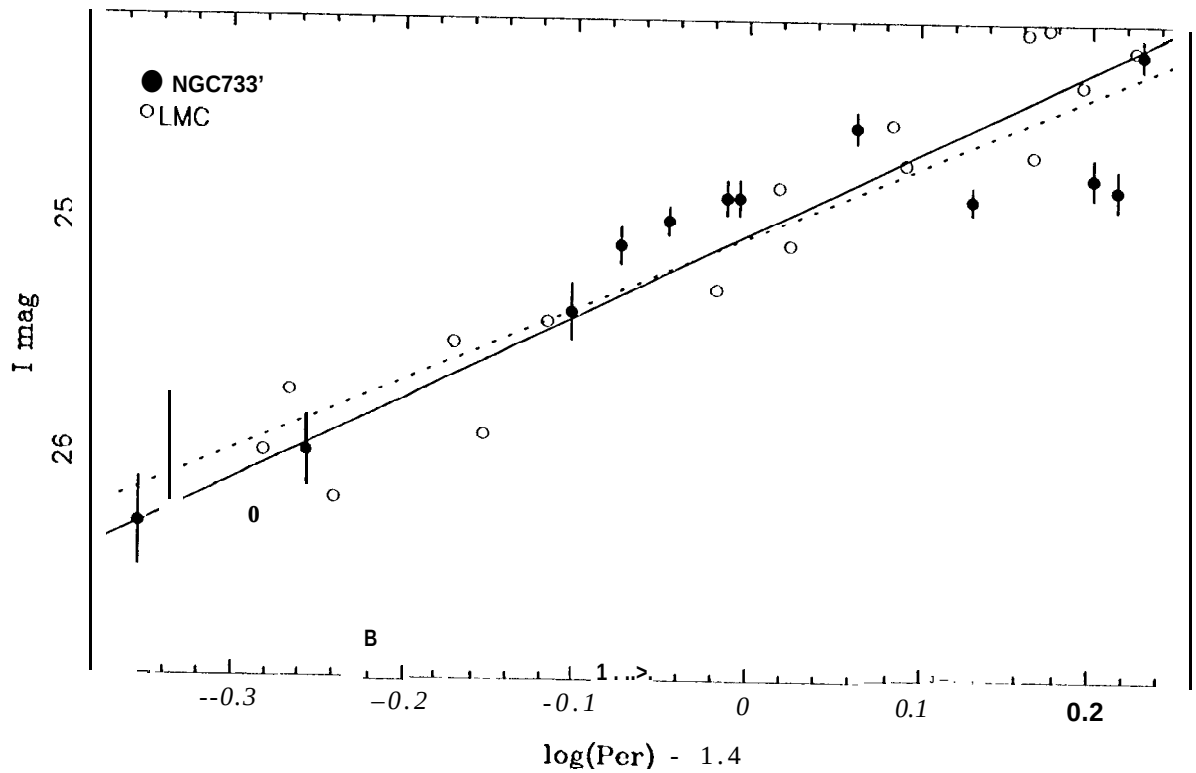
NGC733'
LMC
I mag
25
26
B
1...>
--0.3
−0.2
-0.1
0
0.1
0.2
log(Per) - 1.4

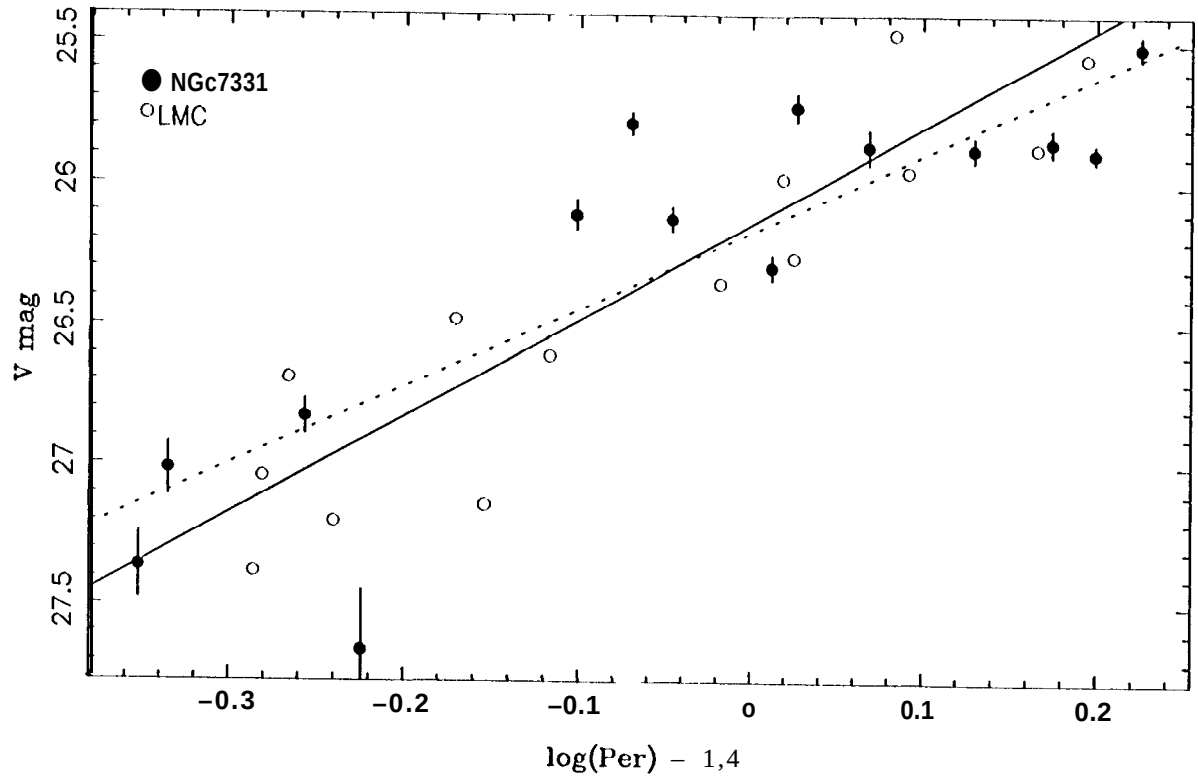
NGc7331
LMC
V mag
25.5
26
26.5
27
27.5
−0.3
−0.2
−0.1
0
0.1
0.2
log(Per) − 1,4

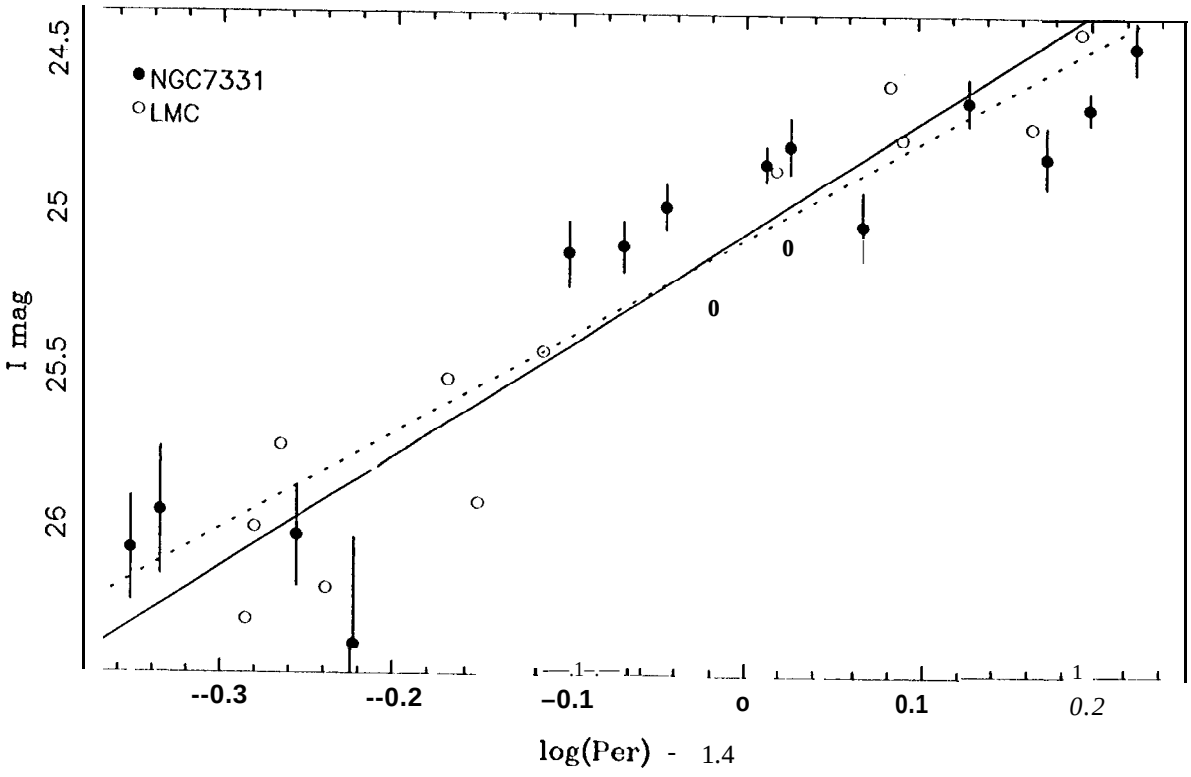
NGC7331
LMC
I mag
24.5
25
25.5
26
--0.3
--0.2
−0.1
0
0.1
0.2
log(Per) - 1.4

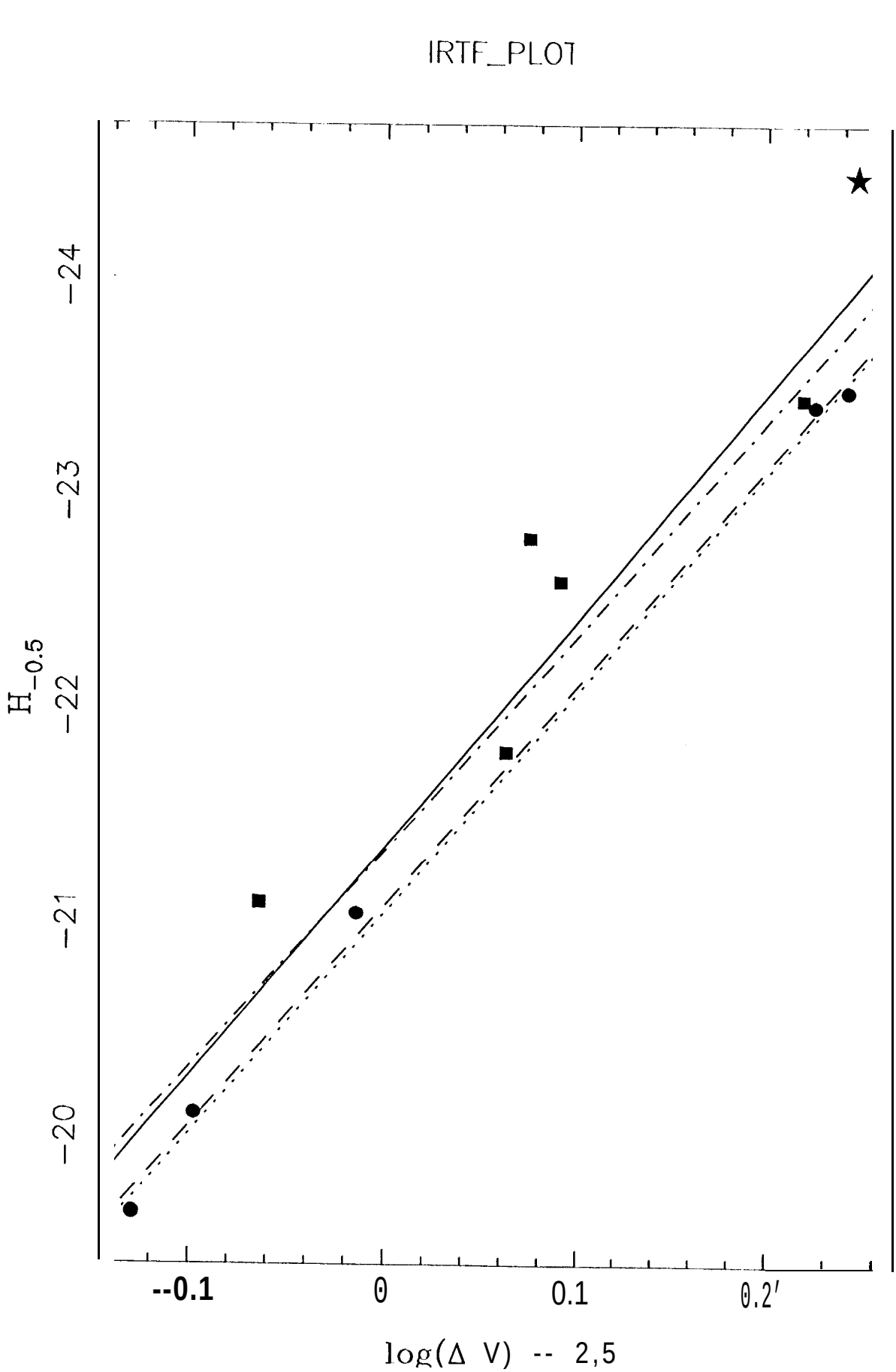
IRTF_PLOT
H_-0.5
-24
-23
-22
-21
-20
--0.1
0
0.1
0.2'
log(Δ V) -- 2,5